Photonic crystal heterostructures and interfaces

Emanuel Istrate* and Edward H. Sargent

*Department of Electrical and Computer Engineering, University of Toronto,
Toronto, Ontario, Canada M5S 3G4*

Photonic crystal heterostructures, like their semiconductor quantum electronic counterparts, generate complex function from simple, well-understood building blocks. They have led to compact photonic crystal-based waveguides and record-quality-factor resonant cavities. Here the progress on the experimental realization of photonic crystal heterostructure devices, and on the development of convenient, intuitive, and computationally efficient models of devices that unite multiple finite-sized photonic crystal media to engineer photon localization and guidance is summarized.

PACS number(s): 42.70.Qs, 73.21.−b, 42.25.Gy, 42.25.Fx

CONTENTS

I. INTRODUCTION

Semiconductor heterostructures are made by combining at least two materials that have distinct band structures. Heterostructures such as quantum wells confine electronic wave particles on the quantum length scale, enabling refined control over electronic states and carrier transport. Heterostructure engineering is now widely practiced, producing the most efficient semiconductor lasers (Tsang, 1982), highest-speed transistors (Hafez and Feng, 2005), and novel quantum electronic devices (Sakaki, 1982; Capasso *et al.*, 1989; Heiblum and Fischetti, 1990).

Photonic crystals (John, 1987; Yablonovitch, 1987)—artificial materials with a periodic modulation of their dielectric constant (Joannopoulos *et al.*, 1995)—display many properties analogous to semiconductors, including the appearance of pass bands, band gaps, and a complex dispersion relation. Early resonant devices based on photonic crystals, however, have differed from the heterostructures typically found in semiconductor devices. The first photonic crystal device proposals and demonstrations were based on much smaller point and line defects.

Recently, photonic crystal heterostructures have been introduced, and they have been shown to extend many of the attractive features of their semiconductor counterparts into the optical domain. Heterostructures have led to low loss photonic crystal waveguides, record resonator quality factors, and high-efficiency add-drop filters. As with semiconductors, photonic heterostructures can be either abrupt or graded.

Semiconductor heterostructures are usually modeled

*Electronic address: e.istrate@utoronto.ca

by separating the spatial variation of the structure into two distinct length scales on which the potential energy varies. Atomic periodicity, with its potential profile undulating on the angstrom scale, produces a band structure conveniently distilled in terms of band edges and effective masses. Individual regions made up of a particular type of crystal, with linear dimensions on the order of multiple nanometers and above, are then treated as quasihomogeneous materials. Semiconductor quantum wells, for example, are reduced to finite-depth square wells.

This intuitively tractable approach, rooted in the mathematics of the multiple scale method, is equally attractive in the case of photonic crystal-based devices that deviate from periodicity. Several such methods have been introduced including envelope approximations, methods based on Wannier functions, tight-binding approximations, and methods based on interface reflection and transmission coefficients.

This article reviews proposed and demonstrated heterostructure devices, along with successful demonstrations of single heterojunctions. Many of the methods used in the design and analysis of heterostructures are also applicable to other photonic crystal structures. For this reason we will review methods used to consider photonic crystals with deviations from periodicity for devices involving both heterostructures and junctions between photonic crystals and other media. At the same time, contrasts and similarities with analogous methods developed for semiconductors will be described.

II. REVIEW OF SEMICONDUCTORS AND PHOTONIC CRYSTALS

Photonic crystal heterostructures form a natural extension to the analogy between semiconductors and photonic crystals. In this section a brief review of semiconductor heterostructures will be given.

Infinitely periodic crystals have attractive features such as a complex dispersion relation that includes allowed and forbidden bands. They are, however, of limited practical use in isolation because, as described by the Bloch theorem, allowed modes propagate much the way plane waves do in a homogeneous medium. To produce a sufficiently functionally sophisticated device, it is necessary to differentiate material properties in space within the heart of a device. The fermionic nature of electrons makes available two methods that can produce such a differentiation in semiconductors: altering the carrier concentration through doping or varying the band structure by changing the semiconducting material. The former produces homojunctions, whose discovery led to the fabrication of diodes and transistors. The latter produces heterostructures.

Semiconductor heterostructures, invented by Herbert Kroemer (Kroemer, 1957, 1963) and Zhores Alferov, have played an essential part in the development of high-speed transistors and semiconductor lasers (Alferov, 2000), earning their inventors the Nobel Prize in 2000. They are formed by the junction of two or more semiconductors in a single crystal (Sharma and Purohit, 1974). By using semiconductors with different band gaps and electron affinities, considerable freedom is obtained in selecting the band arrangements of resulting structures, leading to the concept of band-gap engineering (Capasso, 1992). Moreover, ternary and quaternary semiconductors allow a continuous tuning of the band gap.

Since a heterostructure is composed of multiple semiconductors, it has different band gaps in different regions. Charge carriers in the conduction and valence bands experience different potential energies in different areas of the structure. As a result, heterostructures provide a convenient method to engineer the confining potential for charge carriers, giving rise to many quantum-mechanical structures such as wells and barriers. This forms the basis of most electronic and optoelectronic devices employing heterostructures. A variety of devices have been proposed and demonstrated, as reviewed by Weisbuch and Vinter (1991) and Mitin *et al.* (1999), and summarized below.

One of the simplest structures that can be fabricated using heterostructures is a quantum well, obtained by inserting a low-band-gap semiconductor between two higher-gap materials. Carriers will see a lower potential in the center region, and will be confined there, just like a particle in a finite potential well. Electrons and holes exist in this structure only at certain resonant energies. This band arrangement is used in semiconductor lasers to reduce the energy spread of carriers participating in the gain mechanism. Similar structures form resonant tunneling barriers (Chang *et al.*, 1974), used in transistor structures to select the energy of charge carriers injected across the device (Capasso *et al.*, 1989).

A periodic alternation of two semiconductors forms a superlattice (Esaki, 1986). The name is derived from the fact that the superperiod structure develops its own set of allowed and forbidden bands—known as minibands—on top of the underlying semiconductor bands. Superlattices are therefore used to separate a band of the semiconductor into several minibands. This allows transitions to occur within the conduction band only, or alternatively in the valence band. These intraband transitions have been used with great success in quantum cascade lasers (Capasso *et al.*, 2002), which emit light in the midinfrared region, a range of frequencies where conventional interband transitions are difficult to control for emission.

Heterostructures are also used to improve the high-speed performance of transistors. In bipolar junction transistors, a higher-band-gap material can be used in the emitter compared with the material used in the base and collector regions. It allows the base of the transistor to be doped more heavily while maintaining a good emitter injection efficiency. The higher doping in the base reduces its resistance and gives the transistor a higher cutoff frequency. Such transistors are called heterojunction bipolar transistors (Kroemer, 1982). They are one of the original motivations for the development of the heterostructure (Kroemer, 1957).

The high-frequency response of field-effect transistors can also be increased using semiconductor quantum structures. A channel with a high carrier concentration can be obtained in a lightly doped material by creating a quantum well and doping only the barriers. The charge carriers will be captured by the well, resulting in a channel with the mobility of an undoped material in a region with a carrier concentration similar to that of a heavily doped semiconductor, maximizing both elements needed for a large drift current. Such devices are called high electron mobility transistors (Fritzsche, 1987).

Photonic crystal have many characteristics similar to electronic semiconductors, such as the appearance of bands and band gaps. As is the case with semiconductors, most functional devices rely on careful spatial differentiation of material properties. Photons in a crystal, however, do not have a completely analogous role to electrons. Concepts such as Fermi levels and equilibrium carrier concentrations are not directly extensible to the photonic case. As a result, differentiation of material properties in a device through nonuniform doping cannot be achieved. For this reason, photonic crystal devices use either heterostructures—the subject of this review—or smaller point and line defects.

III. EXPERIMENTAL REALIZATIONS OF PHOTONIC CRYSTAL HETEROSTRUCTURES

Many different methods have been introduced for the fabrication of photonic crystals, some producing two-dimensional and others three-dimensional crystals. Photonic crystal fabrication methods can be divided into three broad categories: micromachining and growth using semiconductor processing techniques (Yablonovitch et al., 1991; Krauss et al., 1996; Robbie et al., 1996; Painter et al., 1999; Lin et al., 2001; Sato et al., 2002; Kawakami et al., 2003; Lidorikis et al., 2004), self-assembly of three-dimensional crystals (Jiang, Bertone, et al., 1999; Kumacheva et al., 1999), and holographic exposure of photoresist (Campbell et al., 2000). Heterostructures have been fabricated successfully with several of these methods.

A. Self-assembly

The fabrication of photonic crystals by self-assembly has become a widespread method, since it produces large volumes of high-quality crystals rapidly (Wong et al., 2003). If made of glass spheres, the resulting crystals are referred to as artificial opals in view of their similarity with natural opals. The fabrication of self-assembled crystals is done in two steps. First, a monodispersed solution of polymer (Lovell and El-Asser, 1997; Kalinina and Kumacheva, 1999) or silica (Stöber et al., 1968; van Blaaderen and Vrij, 1993) spheres is produced in a suitable solvent, such as water or ethanol. Many of the developments in this area have been reviewed by Xia et al. (2000). The spheres are then induced to assemble into an ordered array. A variety of methods exist, but the highest-quality crystals are obtained by assembling the array on a substrate placed vertically in the solution. This is accomplished by convection forces in the meniscus between the solution and substrate. Two-dimensional crystals were first obtained on a horizontal substrate surrounded by a Teflon ring. A dispersion of spheres in water placed inside the ring forms a positive meniscus, with the thinnest layer at the center. During evaporation, the water flux toward the center results in crystal growth starting at this point (Denkov et al., 1993). Later the arrangement was changed to a vertical substrate that is lifted slowly out of the solution, still relying on the positive meniscus to create a two-dimensional crystal (Dimitrov and Nagayama, 1996). The same method was then used to obtain three-dimensional photonic crystals (Jiang, Bertone, et al., 1999). While most self-assembly methods produce crystals oriented along the (111) direction, large defect-free domains of (100)-oriented crystals were obtained recently (Jin et al., 2005).

If desired, the resulting crystal can be inverted by filling the voids between the spheres with various materials, such as silica (Velev et al., 1997; Ye et al., 2002), titania (Wijnhoven and Vos, 1998), zirconia (Schroden et al., 2002), carbon (Yan, Ziou, et al., 2005), and gold (Landon et al., 2003). Many of the results have been summarized by Velev and Kaler (2000). One of the most important classes of materials for infiltration, however, are high-index semiconductors, such as silicon. Their high index of refraction results in a complete photonic band gap in a colloidal crystal (Blanco et al., 2000; Vlasov et al., 2001).

Although point defects can be placed randomly in a colloidal crystal by mixing a small volume of dopant spheres into the monodispersed solution (Vlasov et al., 2001), the controlled placement of defects is more difficult. As a result, research effort has instead concentrated on heterostructures. Large-area line defects were obtained recently through a combination of self-assembly and photolithography (Vekris et al., 2005; Yan, Zhou, et al., 2005). Controlled placement of point defects was also demonstrated recently using a nanoimprinting technique (Yan, Chen, et al., 2005).

Heterostructures are fabricated using self-assembled crystals by repeating the assembly process with different types of spheres (Jiang et al., 2001; Egen et al., 2003; Wong et al., 2003). The first photonic crystal is deposited directly on the substrate. Subsequent crystals use previous layers as a substrate. They differ in the dielectric constant and size of the spheres. An image of a heterostructure in a colloidal crystal heterostructure is shown in Fig. 1.

Heterostructures between self-assembled opals do not require lattice matching at the interface. As a consequence, crystals differing in sphere diameter can be joined in a heterojunction. Sometimes, however, a small gap can appear between the two crystals (Gaponik et al., 2004), which will have an impact on the optical properties of the junction.

Heterostructures have also been produced by modifying a single self-assembled crystal. Through nonuniform infiltration of air voids in the crystal, the band structure
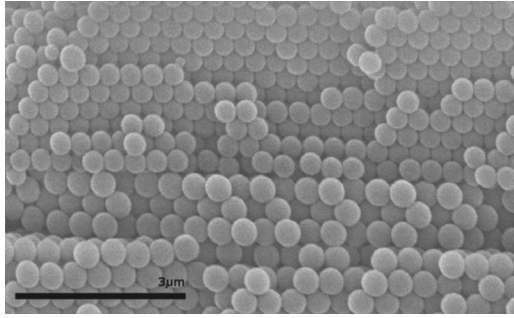
FIG. 1. An example of a heterostructure using colloidal crystals.

can be modified locally. This can be obtained through infiltration only near the surface of the crystal (Romanov *et al.*, 2000). Alternatively, a uniformly infiltrated crystal can be obtained first, which is then patterned. A poly(methyl methacrylate) (PMMA) photonic crystal is first infiltrated with silica. The resulting crystal is then patterned using electron-beam lithography, to which PMMA is sensitive. Upon development, the exposed areas will contain an inverted silica opal, while unexposed areas still contain the PMMA crystal infiltrated with silica (Galisteo-Lopez *et al.*, 2004). Using nonuniform infiltration, photonic crystal heterostructures are obtained with a lattice-matched junction.

B. Autocloning

The autocloning technique is a versatile method used to fabricate three-dimensional photonic crystals for visible and infrared wavelengths (Kawakami, 1997). Alternating layers of two materials, such as silica and tantalum oxide, are deposited on a patterned substrate. Deposition is achieved by sputtering and sputter-etching at the same time. Conditions are chosen in such a way that the substrate pattern is not washed out by subsequent layers, but a periodic modulation is preserved, shown as a cross section in Fig. 2. A three-dimensional crystal is obtained by combining a substrate pattern periodic in two dimensions with alternating layers which are periodic in the third dimension.
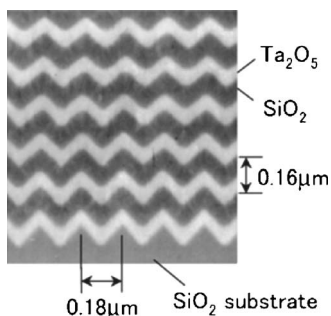
FIG. 2. A photonic crystal fabricated using the autocloning technique. Reprinted with permission from Sato *et al.*, 2002. Copyright 2002, Kluwer Academic Publishers.
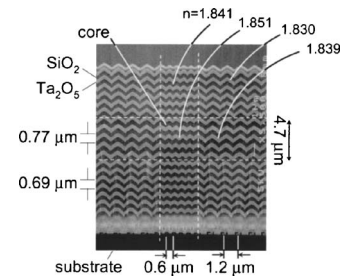
FIG. 3. A photonic crystal heterostructure waveguide fabricated using autocloned photonic crystals. The dashed lines represent the positions of the junctions. Both horizontal and vertical junctions are shown. Reprinted with permission from Kawakami *et al.*, 2003. Copyright 2003, IEEE.

Photonic crystal heterostructures have been fabricated successfully with autocloned crystals. Heterostructures in the horizontal directions are obtained by changing the periodicity of the substrate pattern. Since this pattern is produced lithographically, there is complete freedom in the arrangement of periodic sections. Junctions in the vertical direction are obtained by changing the thicknesses of the two alternating layers (Kawakami *et al.*, 2003). Examples of both cases are shown in Fig. 3. Since horizontal and vertical heterostructures can be combined as desired, optical modes can be completely confined in all three directions in such a device.

C. 2D crystals

The most widely used implementation of photonic crystals are two-dimensional crystals fabricated using lithographic techniques. Usually, a periodic array of holes is etched in a semiconductor slab waveguide. Refractive index guiding is used to keep light in the slab. Triangular lattices are encountered most often, due to the large photonic band gaps that they form, although square lattices are also used. Alternatively, crystals consisting of arrays of dielectric cylinders in air were also demonstrated (Tokushima *et al.*, 2004). Since crystals are defined through lithography, usually electron-beam lithography, there is complete freedom to introduce any deviation from periodicity necessary for device operation. This freedom has been used to fabricate photonic crystals with point and line defects, which act as waveguides and resonators, respectively, as well as combinations of the two.

The lithographic process can also be used to produce photonic crystal heterostructures, by changing the lattice constant, hole size, or even lattice geometry in the crystal. This can be done either abruptly (Song *et al.*, 2003, 2004) or gradually to produce a graded heterostructure (Srinivasan *et al.*, 2003). An example of an abrupt heterojunction is shown in Fig. 4.

It should be noted that graded heterostructures can also be obtained with photonic crystals fabricated by autocloning, and also with infiltrated opals, by slowly varying the infiltration amount.
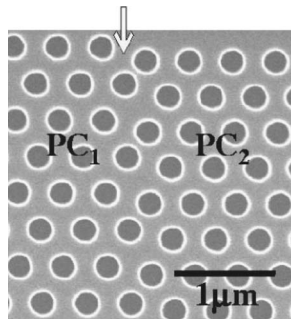
FIG. 4. A photonic crystal heterostructure fabricated lithographically in a semiconductor slab. The arrow shows the position of the junction. Reprinted with permission from Song *et al.*, 2004. Copyright 2004, American Institute of Physics.

FIG. 5. Example of a resonant cavity realized using photonic crystal heterostructures. (a) Refractive index profile. (b) Band diagram. The dashed line represents the frequency of a resonant state.

D. Other methods

For millimeter waves, photonic crystal heterostructures have been fabricated by varying the spacing between directly placed spheres (Yano *et al.*, 2001). Periodic two-dimensional arrays of vertical cavity surface emitting lasers (VCSELs) have also been interpreted as photonic crystals. By changing the periodicity of these crystals, heterostructures were obtained, which were used to control the modes of the laser array (Guerrero *et al.*, 2004).

IV. PHOTONIC CRYSTAL HETEROSTRUCTURE DEVICES

Photonic crystal heterostructures provide the necessary variation in material properties to turn a photonic crystal raw material into a functional device. In particular, they result in a spatial variation of the crystal dispersion relation. Usually, photonic crystal devices are designed in such a way that light at the frequency of interest will encounter a stop band in certain areas and a pass band in others. In this way, the stop bands are used to confine light to certain parts of the device, while the dispersion characteristics of the crystals in the pass bands are used to fine-tune the propagation properties.

Heterostructures, compared to junctions between crystals and other media, have the advantage that the amount of variation between the two crystals can be chosen to be quite small. As shown in this section, this is necessary to achieve certain device properties such as confinement and minimization of radiation losses, especially in two-dimensional crystals. Often, this small variation will necessitate larger device areas than for the usual point and line defects. Heterostructures accommodate this conveniently, as will be seen in the next examples.

A. Resonant cavities

The fabrication of photonic crystal resonant cavities with high-quality factors is one of the most important practical achievements of photonic crystals. The simplest heterostructure cavities are modeled after the semiconductor quantum well and provide a direct demonstration
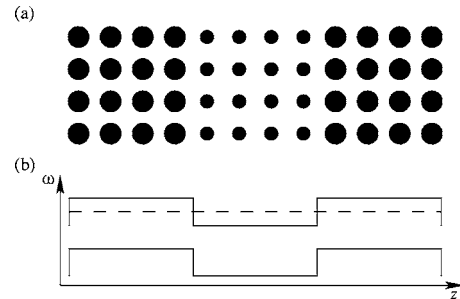
of the quantization of energy levels in a confined system. Using photonic crystal heterostructures, resonant cavities can be obtained by enclosing a thin photonic crystal slab between two crystals with different band gaps, as shown schematically in Fig. 5(a). The two crystals are chosen in such a way that, at the frequency of interest, the center crystal presents a pass band, while the side crystals have a band gap, confining light to the center region. An electromagnetic mode will be allowed in the cavity if it has a frequency corresponding to a resonant state. Using band diagrams similar to those in common use for semiconductor devices, the band alignment and position of the resonant states can be represented as shown in Fig. 5(b).

Resonant cavities are used to select electromagnetic modes of specific frequencies. As such, most photonic crystal heterostructure cavities function like resonant double barriers since the entire structure is embedded in a uniform medium where light propagation is allowed. This medium also contains the optical source and detectors. Light will not be able to traverse the barrier crystals unless it can resonate in the center well, at which point it will tunnel resonantly through both barriers. The transmittance through the entire device reaches unity, similar to the transmittance through a Fabry-Perot etalon. The width and strength of the barriers determine the quality factor of the resonator and corresponding transmission linewidth.

Photonic crystal heterostructure cavities have been used to demonstrate a record-level quality factor of 600 000 (Song, Noda, *et al.*, 2005). The structure is fabricated using two-dimensional photonic crystals in a semiconductor slab. The cavity is formed by a photonic crystal waveguide traversing two heterojunctions, so that light is only allowed in the center section of the waveguide. No waveguide mode exists at that frequency in the barriers. Heterostructures are employed rather than point defects in order to engineer the reflecting properties of the barriers. It was found that a gentle confinement of the mode in the cavity leads to a reduction of the field components with a propagation vector that can radiate out of the slab. A Gaussian profile of the field envelopes is ideal. In earlier attempts, holes surrounding a point defect were moved in order to provide the gentle

confinement, leading to quality factors of 45 000 (Aka-hane *et al.*, 2003). The Gaussian profile was not achieved, however. By using a heterostructure with the well and barrier crystals almost identical, a nearly ideal mode profile was obtained. It was found that the dispersion relation for the imaginary part of the propagation vector in the barriers is highly nonparabolic, approximating a step function. This leads to strong attenuation at frequencies close to the band edge, resulting in a small increase of the modal volume compared to a point-defect cavity and high-quality factor at the same time.

As was already known from semiconductors, photonic crystal heterostructures can be either abrupt or graded. In a graded structure, the crystal properties vary smoothly, with no apparent discontinuity. Resonant cavities based on graded heterostructures have also been demonstrated, again taking advantage of the many degrees of freedom available to optimize the resonator quality factor (Srinivasan, Barclay, and Painter, 2004). A quality factor Q of 40 000 was obtained.

Photonic crystal heterostructure resonators have also been used with periodic VCSEL arrays (Guerrero *et al.*, 2004). The confinement properties of the resonator were used to control the intensity of each VCSEL in the array, giving a direct optical image of the cavity modes, and of the similarity between photonic crystal resonators and semiconductor quantum wells. More recently, coupling between two heterostructure cavities was demonstrated in a similar structure (Lundeberg *et al.*, 2005).

B. Waveguides

Photonic crystal waveguides are a special case of resonant device, where light is confined in two lateral directions, and is allowed to propagate in the third direction. Traditionally this was achieved by placing line defects in an otherwise uniform crystal. Photonic crystal heterostructures, however, are also suitable for this function. The required structure is again similar to that shown in Fig. 5(a). Light in the center crystal, which acts as the core, will be blocked by the side claddings, and can only propagate in the vertical direction. Here again, photonic crystal heterostructures have the advantage of offering more degrees of freedom in tuning the dispersion relations of both the core and cladding. As a consequence, single-mode propagation can be obtained in a guide with a wider core, allowing more efficient end coupling to the waveguide.

One of the first demonstrations of high transmission through a photonic crystal waveguide used heterostructures (Lin *et al.*, 2000) with two-dimensional triangular photonic crystals of air holes in a GaAs slab. The waveguide core is made of a three-period-thin photonic crystal, surrounded by claddings which are made of two crystals with smaller holes. As is usually the case for photonic crystal waveguides, the claddings present a band gap at the wavelength of operation, while the core allows propagation. As mentioned above, the waveguide was made wide enough, which helped efficient coupling
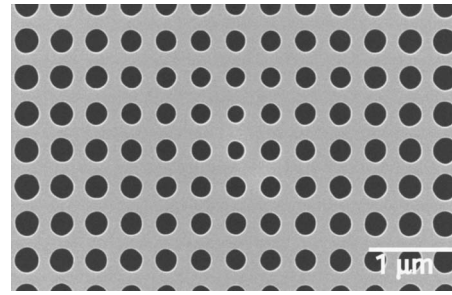
FIG. 6. A graded photonic crystal resonator. Reprinted with permission from Srinivasan, Barclay, and Painter, 2004. Copyright 2004, Optical Society of America.

to conventional waveguides. A homogeneous core of this width produces a waveguide with a large number of modes. Using the heterostructure, the confinement of the mode in the core is made weaker, such that even the wide core used only leads to three modes. The guide can operate as a single-mode guide over significant frequency ranges. The increased width of the core reduces both coupling and radiation losses, reaching a guiding efficiency of 100% at certain frequencies.

Autocloned photonic crystal heterostructures, such as the cross section shown in Fig. 3, can be used to produce photonic crystal waveguides (Kawakami *et al.*, 2003; Miura *et al.*, 2003) that use photonic stop bands to confine light in all three directions. This reduces losses due to leakage out of the plane. As before, the use of heterostructures allows a much wider core and reduces coupling losses to other waveguides. Autocloned waveguides also have the advantage that the periodicity of the crystals can be reduced to two or even one dimension in parts of the device where full 3D periodicity is not necessary. This can be done, for example, in the core of the waveguides, and reduces scattering losses.

C. Graded heterostructure cavities and waveguides

While the above examples have covered abrupt heterostructures, graded heterostructures have also been employed in waveguides and resonators. Fabrication has been demonstrated using two-dimensional crystals etched in semiconductor membranes. The graded structures, such as the one shown in Fig. 6, minimize radiation losses in resonant cavities (Srinivasan, Barclay, and Painter, 2004; Srinivasan, Barclay, *et al.*, 2004), by reducing the intensity of the mode components with momentum values below the light line. Grading of the crystal parameters along a line-defect waveguide was used to design waveguides optimized for evanescent coupling to optical fibers (Barclay *et al.*, 2003), and in order to localize light in certain sections of the guide (Baba *et al.*, 2004).

D. Other structures

Other than the formation of resonant cavities and waveguides, junctions between photonic crystals can

also be used for a number of other purposes. An array of photonic crystals of differing lattice constants with a point defect in each section was used as a multichannel add-drop filter (Song *et al.*, 2005b). The varying lattice constant resulted in a different resonant wavelength in each defect, while maintaining similar quality factors. A waveguide traversing all photonic crystal sections was used to couple light to the point defects. Heterostructures are also used as wavelength-selective mirrors. A line-defect waveguide traversing this heterojunction will have different cutoff frequencies on two sides of the junction, resulting in a wavelength-dependent reflection coefficient. This was used to improve the efficiency of add-drop filters using point-defect resonators. Normally, the efficiency of these filters is limited to either 50% or 25% since some of the light coupled from a waveguide to the resonator will couple back. The wavelength-selective heterostructure reflector can be used to reflect this light back to the point defect (Song *et al.*, 2005a). A drop efficiency higher than 80% was demonstrated (Takano *et al.*, 2005).

A cascade of photonic crystal heterostructure resonant cavities leads to a photonic superlattice, with its own set of allowed and forbidden minibands (Istrate *et al.*, 2002). These can be used to engineer complex optical filtering functions. Colloidal photonic crystal heterostructures have been used to fabricate such photonic superlattices by alternating the growth of two photonic crystals (Rengarajan *et al.*, 2001). The separation of the individual photonic bands into miniband pass and stop bands, expected from semiconductor superlattices, was observed.

Junctions between different photonic crystals also appear naturally when waveguides with different orientations are needed. Photonic crystal lattices only allow line-defect waveguides to be fabricated in a very small number of directions. Lattices of different symmetries, however, allow waveguides in different directions. Multiple cladding crystals can be used, with the waveguide crossing from one to the other as needed, in order to accommodate the necessary bends in a photonic circuit (Sharkawy *et al.*, 2002).

Junctions between crystals of different dimensionality have also been proposed (Chutinan *et al.*, 2003; Chutinan and John, 2004). It is well known that three-dimensional photonic crystals can exhibit a complete band gap and inhibit propagation in all directions. Two-dimensional crystals do not have this ability. They can be processed, however, with better control especially when small defects must be introduced. It would, therefore, be beneficial to enclose an optical circuit fabricated in a two-dimensional crystal between two three-dimensional crystals, in order to reduce the out-of-plane loss inherent in most two-dimensional implementations.

Finally, photonic crystal heterostructures have also been proposed for the simple task of increasing the width of stop bands. By cascading photonic crystals with slightly different stop bands, a structure with a wider effective stop bandwidth is obtained (Zhang *et al.*, 2000;

Wang *et al.*, 2002), in a way similar to the use of chirped gratings for wide-band reflectors in optical fibers.

E. Similarities and differences from semiconductors

A surprisingly high number of similarities has been found between photons, governed by the wave equation, and electrons obeying Schrödinger's equation, due in large part to the similarities between these two equations. Differences appear, however, as a consequence of the fermionic nature of electrons and bosonic nature of photons, and also because electrons have a scalar wave function compared to vectorial photons. It is interesting to note, however, that the vectorial properties of photons lead to two orthogonal polarizations, analogous with the two spins of electrons (Bhandari, 1990).

The analogies between photons and electrons have been investigated in detail (van Haeringen and Lenstra, 1990). For photonic crystals, the fundamental analogy is between Anderson localization of electrons (Anderson, 1958) and localization of light in disordered media (John, 1987).

Several pairs of analogous experiments have been performed on electrons and photons. The quantized conduction of point contacts has been observed for electrons in a two-dimensional electron gas (van Wees *et al.*, 1988) and for photons in a narrow slit (Montie *et al.*, 1991). Tunneling of electrons between two neighboring semiconductor quantum wells has been observed through its submillimeter wave emission (Roskos *et al.*, 1992). Its optical equivalent—coupling of light between two parallel waveguides (Yariv and Yeh, 1984)—is widely used in many optical systems. Bloch oscillations have been observed for electrons in semiconductor superlattices (Feldmann *et al.*, 1992; Waschke *et al.*, 1993). A similar effect is predicted for photons in chirped Bragg gratings (Wilkinson, 2002), chirped photonic crystals (Malpuech *et al.*, 2001), and in arrays of curved optical waveguides (Lenz *et al.*, 1999).

One must be careful, however, in observing the limits of the analogies between electrons and photons. Semiconductor resonant double barriers (Chang *et al.*, 1974) are widely assumed to be analogous to the optical Fabry-Perot interferometer. Space-charge buildup in the electronic device, however, leads to hysteresis in the current-voltage relationships (Eaves, 1990), which does not exist in the optical equivalent. This example shows that electron transport results in changes in the energy bands. Such changes in energy levels due to the movement of charge carriers also affects band alignments and band offsets at a junction. In semiconductors, the energy levels on two sides of a junction influence each other through the process of reaching thermal equilibrium between the two carrier populations. The band offsets can be changed by doping the materials, which sets up slopes in the bands in order to return to a constant Fermi energy. A balance must form between the tendency of carriers to diffuse away from regions of high concentration and resulting electrostatic forces which oppose this diffusion. This is the well-known effect that gives rise to a

built-in potential in *p-n* junctions. The situation is different in photonic crystals where the absolute positions of bands are determined by the crystal periodicity and refractive indices.

Electrons in semiconductors are constantly exchanging energy with the lattice through collisions. Thermalization is an important aspect in the operation of most electronic devices. It is possible for electrons to change energy levels, and jump from one band to another. This allows, among others, the injection of current into a quantum-well laser over the barriers of the well. Electrons will be captured by the well and will relax into its lowest level.

The motion of photons, however, is more closely related to ballistic electron transport. Photons do not usually exchange energy with the surrounding material, except through emission and absorption or through nonlinear interactions at high intensities. As a result, the frequency of light in a heterostructure will normally not change. One must inject light at the frequency of interest in a device. As was mentioned above, however, the acceleration of waves in Bloch oscillation experiments can be simulated through chirping of the optical lattice (Wilkinson, 2002).

V. MODELING AND DESIGNING PHOTONIC CRYSTAL HETEROSTRUCTURES

A. Methods for infinitely periodic and arbitrary structures

Analysis and design of photonic crystal devices is usually done using numerical methods. A few analytic approximations exist for evaluating the position and width of stop bands in one-dimensional photonic crystals. Even when using computers, numerical simulations of photonic crystals are challenging since the entire device to be simulated consists of many photonic crystal unit cells. Each cell must be represented with high accuracy in both its shape and position.

Photonic crystal modeling tools can be divided into three broad categories. Methods in the first category assume an infinitely periodic crystal, for which they compute the band structure and Bloch modes. In the second category are general electromagnetic solvers that find the transmittance and reflectance or resonant modes of arbitrary structures. In the third category are more efficient methods developed for specific photonic crystal configurations.

The methods in the first category are fairly efficient, since only one photonic crystal unit cell needs to be represented. They provide the positions of pass and stop bands, and are often used to obtain rapidly information about the general behavior of the crystals, such as the frequency ranges where light is allowed or forbidden, as well as the dispersion encountered by a wave. Since they are based on the assumption that the crystal is infinite, however, they cannot be used for the accurate simulation of most photonic crystal devices, which are of finite size and contain deviations from periodicity.

The most common algorithm to compute photonic band structures is the plane-wave-expansion method (PWEM) (Ho *et al.*, 1990; Busch and John, 1998). The dielectric profile of the crystal is expanded in a two- or three-dimensional Fourier series. The electromagnetic mode is expressed as a superposition of plane waves. Inserting these two elements into the wave equation transforms it into a matrix eigenvalue equation with the mode frequencies as the eigenvalues and mode profiles as the eigenvectors.

Band structures can also be found using the finite differences in time domain (FDTD) method by finding resonant states when applying periodic boundary conditions with a complex phase shift (Chan *et al.*, 1995). The band structure has also been calculated using transfer matrix methods (Pendry, 1996). While the preceding three methods are applicable to any implementation of photonic crystal, other methods have been developed for more specific cases, such as a scattering matrix method based on Korringa-Kohn-Rostoker (KKR) techniques for photonic crystals made of spheres (Stefanou *et al.*, 1992, 2000).

The methods in the second category have the freedom to represent arbitrary structures, and are therefore the tools of choice for photonic crystal devices, such as waveguides or resonators. They are also able to compute the response of photonic crystal heterostructures. Since they ignore the periodicity of the crystal, however, they are quite inefficient, requiring significant computational resources. This is especially true for heterostructures, where large periodic areas are found often. The most widely used tool in this category is the FDTD method (Yee, 1966; Taflove and Hagness, 2000), which is based on a discretization of Maxwell's equations on a finite grid.

Arbitrary structures can also be considered using the transfer matrix method. Originally developed for one-dimensional problems (Yeh, 1988), it has also been extended to higher dimensions (Pendry and MacKinnon, 1992; Bell *et al.*, 1995). The structure is divided into homogeneous units, with the electric and magnetic fields represented on a fine lattice. Transfer matrices are used to relate fields on neighboring planes in this lattice. As with FDTD simulations, the transfer matrix equations can be used together with the Bloch theorem to yield an eigenvalue problem for the band structure of a crystal.

It should be noted that most methods used to find the band structure of crystals can also be used to find the modes of photonic crystal waveguides and other resonant cavities, by introducing a periodic supercell (Johnson *et al.*, 1999). In directions without periodicity an artificial periodicity is introduced, with a period larger than the dimensions of the mode confined in the resonator. The artificial periodicity makes it possible to represent the structure with a spatial Fourier series, while large periods ensure that resonators will not be coupled together. Therefore, the modes of the periodic array of resonators will be the same as the modes of an isolated resonator.

The PWEM deployed on a supercell belongs to the second category, since the periodic unit is made large enough to cover the entire device. The method is, however, more efficient with structures that are naturally periodic in one or two dimensions, such as waveguides. In such cases, the artificial periodicity is introduced only in directions where natural periodicity is missing.

The third category is a result of the effort to find methods that are more efficient than those in category two, but do not have the requirements of infinite periodicity from the first category. These methods usually impose restrictions on the types of structures that can be considered. For example, they may only be applicable to a certain type of photonic crystal, or may be limited to certain types of defects. The following subsections will present a survey of such methods.

While the discussions in the previous sections have concentrated on photonic crystal heterostructures, many of the modeling tools are applicable to devices using both heterostructures as well as point or line defects. As a result, this review includes methods applicable to both types of photonic crystal devices.

Due to the striking similarity between semiconductors and photonic crystals (van Haeringen and Lenstra, 1990; Gaylord *et al.*, 1993), many of the analysis methods for semiconductor devices have been transferred to the photonic case. A review of the relevant analysis methods developed for semiconductor quantum structures is given in Sec. V.H.

B. Transfer, scattering, and *R*-matrix methods

A large number of methods has been introduced based on transfer and scattering matrices. Common to all of them is the representation of the device as a set of adjacent parallel layers, with the relationship between fields on the two sides of the layers described by a matrix equation. Neighboring layers can be combined by combining their matrices, the end result being a matrix relating fields on the two sides of the new larger layer. This is repeated until a matrix is found that relates fields on the two sides of the entire device. In this discussion, the parallel layers will be assumed to lie in the *x-y* plane, and the evolution of the fields in the *z* direction will be investigated.

The most common method is the transfer matrix method (Pendry, 1996) mentioned already in Sec. V.A for arbitrary structures. In the *x-y* plane, fields are stored on a rectangular grid for each layer of the structure. Transfer matrices are used to relate fields on adjacent layers. This method can be described as belonging to the third category, as well as to the second one, because transfer matrices can be obtained for layers corresponding to one photonic crystal period in the *z* direction. With such matrices, results for large photonic crystal volumes can be obtained quickly by repeatedly applying this matrix. A different matrix is only needed where deviations from periodicity are encountered. Periodic sections of the crystals are therefore considered in an efficient manner, while deviations from periodicity

are permitted. The matrices provide the reflection and transmission spectra directly, or can be used to find the resonant frequencies and mode shapes of resonant structures (Yeh, 1988).

The transfer matrix method (TMM) described above represents the dielectric constant and fields in real space, as opposed to reciprocal space, in all three directions. This gives it the greatest flexibility to consider arbitrary structures. An alternative implementation of the TMM continues to describe the structure in real space along the *z* direction. In the *x-y* plane, however, the structure is expressed in Fourier, or reciprocal, space (Li and Lin, 2003). This assumes that the structure is perfectly periodic in the *x* and *y* directions: each layer behaves like a two-dimensional diffraction grating, diffracting each incident wave into a number of directions, both transmitted and reflected. The transfer matrices relate the incident and diffracted waves on the left-hand side of the layer to the incident and diffracted waves on the right-hand side. Rather than storing fields on a grid in the *x-y* plane, as is done by the real-space TMM, the amplitudes and phases of the different diffraction orders are stored.

Matrix-based methods can be used to compute the response of photonic crystal heterostructures directly (Jiang, Niu, and Lin, 1999). Furthermore, for planar and parallel heterointerfaces that preserve the lattice periodicity, reciprocal-space methods can be used in an efficient manner. These methods can also be used to decouple the interaction between different areas of a device. By representing the field profiles in each layer as a superposition of waves with a component of their propagation vector in the positive *z* direction, and some in the negative *z* direction, it is easy to separate the incoming and reflected waves from a section of the device. This makes it possible, for example, to calculate the reflection coefficients from semi-infinite photonic crystals (Li and Ho, 2003). Such coefficients are very useful in the intuitive understanding of photonic crystal devices, as will be discussed in detail in Sec. V.F.3.

Transfer matrix methods often suffer from stability problems when applied to thick photonic crystals. Wave propagation in the transfer matrix approach is described using familiar complex exponentials. Evanescence in stop bands, however, is given by real exponentials, both positive and negative. Positive exponentials pose stability problems. Over the width of a photonic crystal, they can amplify near-zero field amplitudes, which appear due to numerical errors, to very large, unphysical, values.

A number of variations on the transfer matrix have been proposed to eliminate the stability problems. A comparison of some of these has been published (Li, 1996). One solution is to replace the transfer matrix by a scattering matrix. The transfer matrix relates fields on one side of a layer to fields on the other side. With scattering matrices, the incident waves on a layer from both sides are related to the outgoing waves. In the scattering matrix framework, layers cannot be simply combined by matrix multiplication, but recursive algorithms exist for

this purpose (Li, 1996). In return, exponential terms are avoided in the matrices, leading to a stable algorithm (Li and Ho, 2003; Li and Lin, 2003).

The *R*-matrix methods are similar in concept. They use a matrix to relate the electric fields on both sides of a layer to the magnetic fields. The matrix, therefore, represents an impedance of layers. As with the TMM, fields in the *x*-*y* plane have been represented in both reciprocal space (Elson and Tran, 1995) and real space (Elson and Tran, 1996). In a similar way to the scattering matrix method, the *R*-matrix method does not have stability problems due to exponentially growing components.

For photonic crystals made of arrays of spheres, scattering and transfer matrices can be calculated efficiently using KKR-based methods (Stefanou *et al.*, 1992, 1998; Yannopapas *et al.*, 2001). The scattering of light from each plane of spheres is computed analytically, using spherical harmonics, while interactions of waves scattered by each plane are calculated using transfer or scattering matrices.

C. Calculation of interface states

Interfaces are an important part of many photonic crystal devices, based both on heterostructures as well as point and line defects. In heterostructures, heterointerfaces appear at every junction. In line-defect devices, such as waveguides, interfaces between photonic crystals and homogeneous materials appear at the junctions between the core and claddings. Most resonant photonic crystal devices do not rely on interface states directly; confinement is formed instead by pairs of photonic crystal reflectors. Interface states do appear, however, under certain circumstances. These are states bound to the interface between two semi-infinite materials. They decay exponentially in both of these materials. In the cases presented here, either one or both of these materials is a photonic crystal.

Interface states can affect strongly the transmission of light between two media. It was found that these states can be used to overcome the diffraction limit for light emerging from an aperture of the same size as the wavelength (Kramper *et al.*, 2004; Moreno *et al.*, 2004). It is therefore important to know the frequency bands where such states appear, their dispersion relations, and mode profiles. Bound surface modes are also important for many devices, due to the possibility of light coupling from nearby waveguides into these modes. Such coupling was investigated theoretically in a two-dimensional photonic crystal of air holes (Lau and Fan, 2002), between a double-trench photonic crystal waveguide core and neighboring photonic crystal surfaces. Later measurements of the waveguide transmission (Vlasov *et al.*, 2004) were found to be in good agreement with the dispersion of surface modes.

Interface states between a photonic crystal and homogeneous material were first studied (Meade *et al.*, 1991) for a three-dimensional *Yablonovite* crystal (Yablonovitch *et al.*, 1991). The analysis was done with a plane-wave method on a supercell. Such states must have propagation vectors that are large enough to prevent radiation into air. Their frequency must correspond to a photonic crystal band gap to prevent radiation into the crystal. Besides these conditions, interface modes were found to be dependent on the interface properties, in particular on the position in the unit cell where the interface is placed. Bound interface states do not appear for every surface termination, but at any frequency bound states will appear at least for some terminations. Similar simulations for two-dimensional crystals of dielectric rods in air have found surface modes only if the crystal is terminated with a plane that cuts through the cylinders. This was confirmed experimentally (Robertson *et al.*, 1993) at microwave frequencies using a prism coupling setup to excite surface modes. For crystals of air cylinders etched in a dielectric, surface modes were found even when the interface plane does not cut through the cylinders (Ramos-Mendieta and Halevi, 1999).

Similar simulations were performed for heterointerfaces between two different two-dimensional photonic crystals (Lin and Li, 2001). Again a supercell of two crystals was considered using a plane-wave expansion. It was found that heterostructures formed by changing the filling fraction of the crystals while maintaining lattice matching do not support states. States may appear, however, if two crystals are shifted with respect to each other by half a lattice constant, or if they are separated from each other by a similar amount.

Previous simulations on a supercell require significant computing resources, due to the large cells that must be considered. One of the most important parameters for these modes, however, is the decay length into the crystal. This decay length can be obtained directly from the complex band diagram of crystals in the band gap (Stefanou *et al.*, 1992; Suzuki and Yu, 1995; Hsue *et al.*, 2004; Istrate *et al.*, 2005). This will be described in more detail later.

D. Envelope approximations

The envelope approximation is used often for the analysis of semiconductor heterostructures, since it allows such devices to be understood with quantum-mechanical methods developed for much simpler quantum structures, without taking into account intricate details of the crystalline atomic potential. An effective Schrödinger equation is obtained in which confining potentials are determined by band offsets at the heterojunctions. The energy states of electrons in the heterostructure are then obtained from these equations, in which there remains no explicit dependence on the potential variations on the scale of the crystal lattice period. Phenomena accessible in this approximation include quantum-confined discrete quantum-well states, interband and intraband transition matrix elements, resonant tunneling, and the formation of superlattice subbands (Bastard, 1988; Weisbuch and Vinter, 1991; Coldren and Corzine, 1995).

The envelope approximation has been applied successfully to photonic crystal structures. Since it considers the envelope of the potential profile, instead of its fine variation, the results will also only provide the envelopes of modes in the devices, instead of the true wave profiles. This, however, is acceptable in almost all cases, since the envelope gives sufficient information about quantities of interest, such as mode frequencies and quality of confinement.

1. $k \cdot p$ theory in photonic crystals

In the electronic domain, the envelope approximation relies on the $k \cdot p$ theory to calculate band curvatures and from there the effective masses. When using $k \cdot p$ theory, the Hamiltonian for a state in the neighborhood of a propagation vector $\mathbf{k}_0$ is expressed as a perturbation of the Hamiltonian at $\mathbf{k}_0$. The modes are also expressed as superpositions of states at $\mathbf{k}_0$, with the assumption that these states form a complete set. This is indeed so for the electronic case, but is not true for photonic crystals. A larger number of basis states, including some unphysical solutions of the wave equation, must be used in the photonic case, as was found from a rigorous $k \cdot p$ theory developed for photonic crystals (Sipe, 2000), summarized here.

The modes of periodic dielectric structures are found from the wave equation (Joannopoulos *et al.*, 1995), written here in terms of the magnetic field,

$$\nabla \times \left(\frac{1}{\epsilon(\mathbf{r})} \nabla \times \mathbf{H}(\mathbf{r}) \right) = \left(\frac{\omega}{c} \right)^2 \mathbf{H}(\mathbf{r}), \tag{1}$$

where $\epsilon(\mathbf{r})$ is the periodic dielectric constant, $\mathbf{H}(\mathbf{r})$ is the magnetic field vector, ω is the frequency of the mode, and c is the speed of light in vacuum.

As opposed to the Schrödinger equation for electrons, which only produces physical solutions, the wave equation also produces some unphysical solutions of zero frequency. The physical solutions must also satisfy the divergence condition, which requires the fields to be transverse,

$$\nabla \cdot \mathbf{H}(\mathbf{r}) = 0. \tag{2}$$

This requirement does not have an equivalent in semiconductor theory where the wave function is scalar.

Photonic crystal Bloch modes form a complete set for the expansion of modes at neighboring propagation vectors only if unphysical solutions are also included (Sipe, 2000). In other words, the entire set of solutions of the wave equation must be used, including those that would normally not be associated with photonic bands.

For numerical calculations, however, where the expansion is truncated to a finite number of basis functions, the zero-frequency solutions can be neglected, since they only provide small corrections, similar to the corrections from other remote bands.

In semiconductors, the $k \cdot p$ theory results in a parameter known as the effective mass, which describes the curvature of the bands, as summarized in Sec. V.H. This parameter has units of mass and determines the accel-

eration of Bloch waves in the crystal under the influence of external forces. For photonic crystals, similar parameters can be extracted from the Bloch modes. In analogy to the semiconductor case, the term "effective" is used sometimes to describe these parameters. In this case, however, these terms are unrelated to a physical mass. They only serve as parameters in the dispersion relation encountered by photons.

2. The envelope equation

In periodic optical structures, the envelope approximation was first used to model the propagation of optical pulses in nonlinear periodic structures (de Sterke and Sipe, 1988). It calculates the response to slow variations in refractive index induced by the presence of an optical pulse, in an otherwise uniform crystal. The approximation was also applied to photonic crystal heterostructures (Istrate *et al.*, 2002). The objective of this technique is to replace the full wave equation, Eq. (1), with an equation that treats each section of the photonic crystal as a uniform material. In other words, the wave equation is manipulated to remove the dependence on $\epsilon(\mathbf{r})$. This dependence will be replaced by effective parameters, similar to the effective mass in the electronic case. Such an equation can be obtained by following a procedure similar to the $k \cdot p$ calculation in semiconductors. The electric field is expanded as a sum of Bloch waves at a chosen $\mathbf{k}$ vector. This expansion is then inserted into the wave equation, leading to the envelope equation

$$\Theta \mathbf{W}_\lambda = \omega_\lambda^2 \mu \mathbf{W}_\lambda. \tag{3}$$

Here $\mathbf{W}_\lambda$ is a column vector whose elements $W_{\lambda,n}$ represent the envelopes of the different photonic crystal bands in the heterostructure. ω_λ is the frequency of the heterostructure mode and μ is the magnetic permeability. The matrix operator Θ has elements

$$\Theta_{n,m} \equiv -\left[\left(\frac{\partial^2}{\partial z^2} + k_{0z}^2 \right) s_{n,m} + \kappa_{n,m} \left(\frac{1}{j} \frac{\partial}{\partial z} - k_{0z} \right) \right.$$
$$\left. - \omega_n^2 \mu \delta_{n,m} \right]. \tag{4}$$

Here the heterostructure is assumed to be perpendicular to the z direction. $k_{0,z}$ is the z component of the propagation vector at which the $k \cdot p$ expansion is performed. It is usually absent in such equations for semiconductors, since the expansion is normally performed at the $k=0$ point, where charge carriers accumulate. In photonic crystals, photons do not accumulate at the band edge. Hence, $k_{0,z}$ must be determined by the frequency of interest in relation to the band structure. $s_{n,m}$ and $\kappa_{n,m}$ are constants derived from the Bloch modes of the infinitely periodic photonic crystals (Istrate *et al.*, 2002). $s_{n,m}$ is obtained in a manner very similar to the effective mass of semiconductors, and plays an analogous role in determining the curvature of the bands, since it is multiplied by the second derivative operator. It should be noted, however, that it is not related to a physical mass. $\kappa_{n,m}$ and the entire term involving the first derivative opera-

tor are new in photonic crystals. It is again a consequence of the nonzero value of $k_{0,z}$, where bands have a finite slope, in addition to the curvature.

Equation (3) can now be solved independently in each periodic section of the heterostructure. Its solutions will be either propagating or decaying exponentials, depending on the presence or absence of a stop band.

3. Envelope boundary conditions

Boundary conditions are required at the junctions, in order to connect the envelope solutions. For dielectric structures, the well-known boundary conditions are the continuity of the wave and its derivative. This is a result of the requirement for continuity of both the tangential electric and magnetic fields, since the magnetic field is proportional to the derivative of the electric field, and vice versa. Such an approach cannot be taken to obtain boundary conditions for heterostructure envelopes, since the two vector fields have been reduced to a single scalar function. Boundary conditions can instead be obtained (Istrate *et al.*, 2002) using a similar method to the one used to derive the familiar quantum-mechanical boundary conditions (Cohen-Tannoudji *et al.*, 1977).

Although the heterointerface separates two different crystals, it does not usually also correspond to a materials interface. As a consequence, the electric fields at the position of the junction are continuous. The envelope of these fields must therefore also be continuous across the interface. Assuming an interface at $z=0$, the continuity is written as

$$\mathbf{W}_{\lambda,A}(0) = \mathbf{W}_{\lambda,B}(0), \qquad (5)$$

In addition to the condition on the envelopes themselves, a condition is also necessary for their first derivatives, in order to satisfy the requirements of a second-order differential equation. The condition to be satisfied by this derivative at the interface is obtained by integrating Eq. (3) from $z=-\epsilon$ to $z=+\epsilon$, and taking the limit of ϵ approaching zero,

$$\lim_{\epsilon \to 0} \int_{-\epsilon}^{\epsilon} \mathbf{\Theta} \mathbf{W}_{\lambda} dz = \lim_{\epsilon \to 0} \omega_{\lambda}^2 \mu \int_{-\epsilon}^{\epsilon} \mathbf{W}_{\lambda} dz. \qquad (6)$$

The right-hand side of Eq. (6) contains a finite function, integrated over a vanishing interval. Hence it approaches zero. The left-hand integral contains terms involving the wave envelope and its first and second derivatives. Assuming that the envelope and its first derivative have no infinite jumps, these two terms vanish, leaving

$$\lim_{\epsilon \to 0} \sum_m \int_{-\epsilon}^{\epsilon} \frac{\partial^2}{\partial z^2} s_{n,m} W_{\lambda,m} dz = 0, \qquad (7)$$

which leads to the condition on the first derivative of the envelope,

$$\sum_m s_{n,m} \frac{\partial}{\partial z} W_{\lambda,m} = \text{const}. \qquad (8)$$

This set of boundary conditions is similar to those for electrons in GaAs/AlGaAs heterojunctions (Galbraith

and Duggan, 1988), where the product of effective mass times the derivative of the wave function must be conserved.

The boundary conditions provide the connection rules for the envelope functions on two sides of the interface. Together with the envelope equation, which provides information about the wave inside the uniform sections of photonic crystals, they describe the behavior of light in the entire heterostructure.

Since only envelopes of both the dielectric constant and modes are considered, however, the exact position of the interface within one unit cell is not taken into account. As such the envelope equations are better suited for calculating colloidal crystal heterostructures, where interface conditions are not controlled perfectly. In later subsections, other methods are presented that calculate the boundary conditions using the exact position of the interface in the unit cell.

4. Other comments

The mode envelope equations, shown above in matrix form, are a system of equations with one equation for each photonic crystal band included in the expansion. It was observed that in many cases at frequencies near the first stop band, where most experiments are performed, a weak heterostructure does not introduce a significant mixing between bands, since the perturbation that it introduces is not strong. As a result, the matrix $\mathbf{\Theta}$ in Eq. (3) is nearly diagonal. This means that the heterostructure supports a number of independent modes, one derived from each band. The other bands only provide small corrections. In many instances the system of equations can be reduced to a single equation, by concentrating on the band at the frequency of interest. The other equations in the system describe modes that will appear at other frequencies, and which usually are of lower interest.

The boundary conditions presented above were for uniform crystals separated by abrupt interfaces. The envelope approximation can also be used with graded heterostructures, where properties of the underlying crystals vary smoothly over many periods. For graded junctions it is not possible to break up the structure into a number of uniform sections. The properties of such crystals vary continuously along with the parameters necessary to compute the envelope, such as the coefficients in Eq. (4). They must be evaluated at a number of points along the structure, and interpolated for all other positions (Istrate and Sargent, 2002). If the variation is small, it is possible to include its effects as an additional slowly varying term $\Delta_s(\mathbf{r})$ in the envelope equation. This, however, leads to a generalized eigenvalue equation.

5. Multiple-scale techniques

The preceding subsections have described the envelope equation, a differential equation to be obeyed by the envelope of the electromagnetic wave. This equation does not depend on the fast variation of the refractive index and can therefore be solved much more easily. In

essence, the envelope equation works by separating two length scales of the problem—the rapidly varying photonic crystal dielectric profile from the slower heterostructure variation. This is part of a general class of problems in differential equations that are usually solved using multiple-scale techniques (Kevorkian, 2000). Developments in the preceding paragraphs were derived in a more intuitive fashion, in a form closely resembling the $k \cdot p$ techniques in solid-state physics. This section presents a summary of the wave equation solution in heterostructures using multiple-scale techniques, which are mathematically more general. Regardless of the method used, equivalent results are obtained. As with the envelope approximation, multiple-scale techniques have been used to model pulse propagation through nonlinear photonic crystals. Results for crystals with an arbitrary number of dimensions were obtained (Bhat and Sipe, 2001).

To find the modes of photonic crystal heterostructures using multiple-scale techniques (Poon *et al.*, 2003), coordinates are introduced to represent two length scales,

$$\mathbf{R} = \mu \mathbf{r}, \quad X = \mu x, \quad Y = \mu y, \quad Z = \mu z, \qquad (9)$$

where again the heterostructure varies in the z direction. Here the lowercase variables represent fast features of the structure, while the uppercase parameters represent slower changes. The heterostructure is assumed to be a perturbation to the bulk crystals. The modes and their frequencies in the perturbed structure are expressed as corrections from the bulk values,

$$\omega_n'^2 = \omega_n^2 + \mu \Omega^{(1)} + \mu^2 \Omega^{(2)} + \cdots, \qquad (10)$$

$$\mathbf{E} = \mathbf{e}_0 + \mu \mathbf{e}_1 + \mu^2 \mathbf{e}_2 + \cdots, \qquad (11)$$

where $\Omega^{(i)}$ represent frequency corrections to different orders while $\mathbf{e}_i$ are expansion coefficients of the modes,

$$\mathbf{e}_1 = A(Z)\mathbf{E}_{n\mathbf{k}}, \qquad (12)$$

$$\mathbf{e}_2 = \sum_{l \neq n} B_{l\mathbf{k}}(Z)\mathbf{E}_{l\mathbf{k}}, \qquad (13)$$

$$\mathbf{e}_3 = \sum_{m \neq n} C_{m\mathbf{k}}(Z)\mathbf{E}_{m\mathbf{k}}. \qquad (14)$$

The above equations imply that to the first order of approximation the heterostructure modes are given by bulk modes modulated by an envelope, $A(Z)$. Higher-order corrections use the bulk modes from other bands as well. Truncating this expansion at the second order and using it in the wave equation leads to an equation for the mode envelope and frequency correction,

$$\Omega^{(1)} = 0, \qquad (15)$$

$$\frac{1}{2m_x}\frac{\partial^2 A}{\partial X^2} + \frac{1}{2m_y}\frac{\partial^2 A}{\partial Y^2} + \frac{1}{2m_z}\frac{\partial^2 A}{\partial Z^2} + \Omega^{(2)}A = 0, \qquad (16)$$

where the following definitions are made:

$$\frac{1}{m_x} = \frac{\partial^2 \omega_n^2}{\partial k_x^2}, \quad \frac{1}{m_y} = \frac{\partial^2 \omega_n^2}{\partial k_y^2}, \quad \frac{1}{m_z} = \frac{\partial^2 \omega_n^2}{\partial k_z^2}. \qquad (17)$$

Equation (16) must again be solved in each heterostructure layer separately, and individual solutions matched at the interfaces with appropriate boundary conditions. The parameters m_x, m_y, and m_z represent effects of the infinite photonic crystals on the heterostructure, in a similar way to the use of the $s_{n,m}$ and $\kappa_{n,m}$ parameters from Eq. (3). They are related to the curvature of the bands. As was seen from $k \cdot p$ theory, there is an equivalence between the information conveyed by the shapes of the Bloch modes and curvatures of corresponding bands.

E. Analysis using Wannier functions

1. Wannier-like envelope equations

The envelope approximation has been derived in the previous section using parameters extracted from Bloch modes of the photonic crystals. It is possible to obtain similar information not from Bloch modes, but instead from curvatures of the photonic crystal dispersion relation. This is a phenomenon also encountered in semiconductors. The effective masses of semiconductors are normally defined in terms of the curvature of the bands. Formally, however, they are computed from a $k \cdot p$ analysis which uses the semiconductor Bloch modes instead of the shapes of the dispersion relations. The envelope equations presented in Sec. V.D.2 are very similar to the $k \cdot p$ analysis. The expressions are, however, more complex due to the vectorial nature of the electromagnetic waves and the lack of symmetry in photonic crystal Bloch modes at arbitrary points in the Brillouin zone, as described below Eq. (4).

In the present section, an alternative envelope approximation is introduced that uses band curvatures instead of Bloch modes to parametrize bulk photonic crystals (Charbonneau-Lefort *et al.*, 2002). As before, the goal is to simplify the wave equation to a form that does not include the periodicity of the crystal directly. The starting point is again the wave equation for light in the medium including the fast and slow variations,

$$[\nabla(\nabla \cdot) - \nabla^2]\mathbf{E}_\lambda = \omega^2 \mu \epsilon_f(\mathbf{r})[1 + \Delta_s(\mathbf{r})]\mathbf{E}_\lambda, \qquad (18)$$

where $\mathbf{E}_\lambda$ is the optical mode, $\epsilon_f(\mathbf{r})$ is the fast component of the dielectric constant, and $\Delta_s(\mathbf{r})$ is the slower heterostructure variation. The background dielectric constant is included in ϵ_f. The heterostructure mode is expanded as before in terms of Bloch modes of the bulk crystals,

$$\mathbf{E}_\lambda(\mathbf{r}) = \sum_{n,\mathbf{k}} W_{n,\mathbf{k}} \mathbf{E}_{n\mathbf{k}}(\mathbf{r}) d\mathbf{k}. \qquad (19)$$

$W_{n,\mathbf{k}}$ represents the inverse Fourier transform of the mode envelopes $F_n(\mathbf{r})$ given by $F_n(\mathbf{r}) = e^{i\mathbf{k}_0 \cdot \mathbf{r}} f_{n\mathbf{k}_0}(\mathbf{r})$, assuming they are obtained using a Taylor expansion of the band structure near $\mathbf{k} = \mathbf{k}_0$. In the previous sections, the Bloch modes $\mathbf{E}_{n\mathbf{k}}$ had been expanded in terms of functions at a single propagation vector $\mathbf{k}_0$. This is not done

here, but the above form is used directly in the wave equation, yielding an equation for the envelopes similar to the Wannier equation for electronic states in perturbed semiconductors (Wannier, 1962). Making the same assumptions as before that the heterostructure varies in the z direction only, the equation can be simplified to

$$\frac{1}{2}\left.\frac{\partial^2\omega_n^2}{\partial k_z^2}\right|_{\mathbf{k}_0}\frac{\partial^2 f_{n\mathbf{k}_0}}{\partial z^2} = \{\omega_n(\mathbf{k}_0) - \omega_\lambda^2[1 + \Delta_s(z)]\}f_{n\mathbf{k}_0}(z).$$
(20)

The above equation is for modes in a heterostructure in terms of the curvature of the bands of the bulk crystal. There is one solution for each band. The complete heterostructure mode is given by the summation of bulk modes of each band multiplied by their envelope functions. The above equation neglects band mixing, which was found to be almost nonexistent in many cases, as described in the previous section.

The first term in the envelope equation (20) above contains the curvature of the energy-momentum relation, represented by the second derivative of ω^2 with $\mathbf{k}$. It should be noted that the square of the frequency ω is used, since the $\omega - k$ relationship is normally linear in the photonic case. In analogy with the situation in semiconductors, the curvature is called the effective mass for the photonic crystal,

$$\frac{1}{m^*} = \left.\frac{\partial^2\omega_n^2}{\partial k_z^2}\right|_{\mathbf{k}_0}.$$
(21)

It determines the propagation properties of light in the crystal, in the same way that the effective mass affects electrons in a semiconductor. It is not, however, related to an acceleration.

The envelope approximations shown here and in the previous section have been used to calculate modes in photonic crystal quantum wells and superlattices (Istrate and Sargent, 2002; Istrate et al., 2002), heterostructure waveguides (Charbonneau-Lefort et al., 2002; Poon et al., 2003), and more recently square cavities made of photonic crystals surrounded by homogeneous materials (Xu et al., 2005).

A similar Wannier equation for the envelopes of modes in photonic crystal devices has been derived (Painter et al., 2003) using magnetic fields, taking into account mixing among degenerate satellite extrema of a band edge. This results in a set of coupled eigenvalue equations for the envelopes. These equations were used to compute modes of graded photonic crystal resonators and waveguides.

2. Localized Wannier function bases

The Bloch modes in photonic crystals are expressed often as superpositions of plane waves, which are obtained directly from the plane-wave-expansion method (PWEM) when computing the band structure. Plane waves form a natural basis for representing Bloch modes of infinite extent. Plane waves, however, are inefficient

for representing tightly confined modes in photonic crystal defects. This case appears often in PWEM methods using supercells to calculate point-defect modes. Basis sets formed of localized functions are a more natural choice here. The similarity with semiconductors is again explored in order to find such a basis set, by transferring the tight-binding approximation (Ashcroft and Mermin, 1976) to photonic crystals. When using a localized basis set, bulk photonic crystal modes are first expressed as a superposition of the localized functions, centered on each lattice site. The response of defects is obtained by calculating the eigenmodes of the perturbed structure.

This approximation uses the orbitals of independent atoms as a basis. For atomic crystals, orbitals are naturally confined around each nucleus. Finding a set of atomic orbitals in the photonic case, however, is more complex than in the electronic case, since individual scatters do not produce localized states. Different methods are therefore needed to obtain such a localized set of atomic orbitals. They are normally based on Wannier functions, which can be chosen to be well localized. A review of the different methods has been given by Busch et al. (2003).

In order to find the Wannier functions for bulk crystals, the Bloch modes of the crystals must first be calculated. This is done conveniently using the plane-wave-expansion method. With the bulk Bloch modes known, the Wannier function centered at position $\mathbf{R}$ is given by (Albert et al., 2000)

$$a_m(\mathbf{r} - \mathbf{R}) = \frac{1}{\sqrt{N}}\sum_{\mathbf{k}} e^{-i\mathbf{k}\cdot\mathbf{R}}\phi_m(\mathbf{k},\mathbf{r}),$$
(22)

where N is the number of unit cells, used for normalization, and ϕ_m is a generalized Bloch mode of the photonic crystal. The wave equation in this basis takes the form

$$\sum_{m'}\mathbf{\Theta}_{mm'}(\mathbf{k})U_{m'n}(\mathbf{k}) = \left(\frac{\omega_n(\mathbf{k})}{c}\right)U_{mn}(\mathbf{k}),$$
(23)

where U_{mn} are eigenvectors and

$$\mathbf{\Theta}_{mm'}(\mathbf{k}) = \sum_{\mathbf{R}} e^{i\mathbf{k}\cdot\mathbf{R}}\int a_m^*(\mathbf{r})(-\nabla^2)a_{m'}(\mathbf{r} - \mathbf{R})d^2\mathbf{r}.$$
(24)

The above integrals are considered to be free parameters, which are fitted to the solution of the wave equation, trying to match its results to those from the plane-wave expansion. The resulting Wannier functions are indeed well localized, decaying to nearly zero over one or two lattice constants (Albert et al., 2000).

Instead of computing the Wannier functions using the empirical tight-binding parametrization shown above, the localization of bands can also be optimized by minimizing a spread functional (Souza et al., 2002; Busch et al., 2003).

The field profiles in the defect modes are expressed in this basis as follows:

$$E(\mathbf{r}) = \sum_{m\mathbf{R}} C_m(\mathbf{R}) a_m(\mathbf{r} - \mathbf{R}). \qquad (25)$$

The expansion coefficients C_m can be calculated using the tight-binding method coupled with either Green functions or supercell approximations.

Since the Wannier functions are so well localized, the amplitudes of the expansion coefficients at different lattice sites can be used directly to measure the intensity of the defect modes at different points in the structure.

The localized Wannier function basis can also be used instead of the plane-wave basis to set up a transfer matrix method for two-dimensional structures that are periodic in one direction, but have arbitrary deviations from periodicity in the other one (Albert *et al.*, 2002). Each unit cell of the device is described by a set of Wannier functions related to those in neighboring cells by transfer matrices.

F. Photonic crystal effective medium boundary conditions

The envelope approximation described in the previous sections is an efficient method to compute the response of photonic crystal heterostructures. It requires, however, solutions of an equation different from the wave equation. This section introduces an alternate approach for the analysis of interfaces in photonic crystals, which is very similar to our intuitive thinking about the problem, and also similar to the way in which interfaces between homogeneous dielectrics are normally considered.

The method is best described with the example of a dielectric slab waveguide, composed of a high-index planar core in the x-y plane enclosed by two claddings. Geometric solutions exist for computing resonant modes in such a structure. In each one of the three layers, the field profile is expressed in terms of infinite material modes. In the uniform materials assumed here, the modes will be plane waves of the form $E = E_0 e^{\pm i\mathbf{k}\cdot\mathbf{r}}$, where $\mathbf{k}$ may be complex. These waves are matched at the two core-cladding interfaces. Two conditions must be satisfied at the interfaces. First, the propagation vector of the plane waves in the plane of the interface must be conserved, as required by Snell's law. Second, the boundary conditions of continuity of the electric field and its derivative must be enforced. If these conditions are applied at the two interfaces, it is no longer necessary to solve the wave equation at every point in the device, since the modes of the infinite materials are assumed to be the correct solutions in each layer.

Such an approach is also possible with photonic crystals, if the boundary conditions are provided. This section will review the methods to calculate the boundary conditions. The envelope approximation presented in the previous section, with the boundary conditions derived there, appear to be similar to the approach presented in this section. Here, however, no envelopes will be employed. The true modes of each crystal will be matched at the boundary, resulting in a simpler solution.

At an interface between homogeneous dielectrics it is well known that for each incident wave a reflected and transmitted wave will be generated, with the possibility that the transmitted wave is evanescent. These waves are modes of the infinite material. If the propagation vector of the incoming wave is known, Snell's law can be used to find the allowed propagation vectors for the new waves. Hence, for photonic crystal interfaces the first step would be to find the equivalent of Snell's law. Once the propagation or evanescent decay vectors are found, the amplitudes and phases of the waves propagating with these vectors must be calculated. This is equivalent to the information provided by the Fresnel coefficients for dielectric structures. Their equivalent for photonic crystals must also be found. These two steps are described in the following two subsections.

1. Snell's law equivalent

For homogeneous materials, Snell's law is based on the requirement that all waves at an interface have the same propagation vector in the plane of the interface. This ensures that the wavefronts have the same periodicity on the two sides of the interface,

$$\mathbf{k}_\parallel^A = \mathbf{k}_\parallel^B \equiv \mathbf{k}_\parallel. \qquad (26)$$

The superscripts A and B denote two sides of the interface. Besides this condition, the dispersion relations of the two materials must be obeyed, which give the allowed propagation vectors for each frequency. For homogeneous materials, this is

$$\left(k_\perp^A\right)^2 = \left(\frac{n_A\omega}{c}\right)^2 - |k_\parallel|^2, \qquad (27)$$

$$\left(k_\perp^B\right)^2 = \left(\frac{n_B\omega}{c}\right)^2 - |k_\parallel|^2, \qquad (28)$$

where n_A and n_B are the indices of refraction of the two materials. Using these relations, $\mathbf{k}^B$ can be calculated if $\mathbf{k}^A$ is given.

A similar approach can be taken with photonic crystals, to calculate the propagation vector of photonic crystal Bloch modes leaving the interface, in response to an incoming wave (Notomi, 2000, 2002). Equation (26) is relaxed to allow propagation vectors to differ by a reciprocal-lattice vector. Equations (27) and (28) cannot be applied directly, but similar conditions can be found from the crystal band diagram: the unknown perpendicular propagation vector component, together with the fixed parallel component, must result in an allowed state at the given frequency. In other words, the perpendicular component is found by computing the equifrequency surface of the crystal, and searching for points on this surface with the required parallel wave-vector component.

It should be noted, however, that the direction of the propagation vector obtained with the above analysis is not the direction of power flow in the crystal. Power flows in the direction given by the gradient of the equifrequency surface (Notomi, 2000) at a given point in

k space. Sharp changes in the direction of this gradient are responsible for the superprism effect observed in photonic crystals (Kosaka *et al.*, 1998; Wu *et al.*, 2002). Knowledge of the exact propagation vector will be required, however, in order to evaluate the amplitudes and phases of the modes excited at the interface.

The above analysis was done first for interfaces corresponding to high-symmetry directions in the crystal. It was then extended to cover interfaces in arbitrary directions (Yu and Fan, 2004) by considering equifrequency surfaces in a set of neighboring Brillouin zones. For light incident from the photonic crystal onto an air interface it was also found that in special cases total internal reflection may occur, but in general some light will leave the crystal, again through interaction between the incident wave vector and equifrequency surfaces in remote Brillouin zones. This happens even if the incident wave is below the light line in the first Brillouin zone.

2. Reflection, transmission, and diffraction coefficients found using the complex plane-wave expansion method

The preceding subsection describes methods to calculate which modes could be excited at an interface, or, in other words, the allowed directions for scattered waves. This subsection and the following one describe methods to calculate the amplitude and phases of these modes. These determine how much optical power is transmitted across the interface and how much is reflected. The parameters to be computed are the equivalent of the well-known Fresnel reflection and transmission coefficients for dielectric interfaces. The photonic crystal surface, however, may diffract light into multiple directions. Inside the photonic crystal, light of a single frequency may also excite multiple propagating and decaying modes. For these reasons, the Fresnel coefficients are conveniently expressed as a set of diffraction coefficients, relating each wave incident on the interface to diffracted waves.

For generality, the diffraction coefficients are computed at an interface between a homogeneous dielectric and a photonic crystal. Heterostructures between two photonic crystals can then be represented as a three-layer structure with a thin homogeneous layer between the two crystals. Airy formulas are then used to account for multiple reflections in this layer. Setting the thickness of the homogeneous layer to zero provides the response of the heterostructure. The diffraction coefficients can be computed using two methods, starting either with the Bloch modes of the crystal or with a transfer matrix representation of the structure. The first method will be summarized here while the second one is the subject of the next subsection.

When using the Bloch modes of the crystal, the boundary conditions are found by matching modes of the structures on two sides of the interface. In the photonic crystal, modes are the propagating or decaying Bloch waves described below. On the other side of the interface, modes are usually plane waves. At the inter-
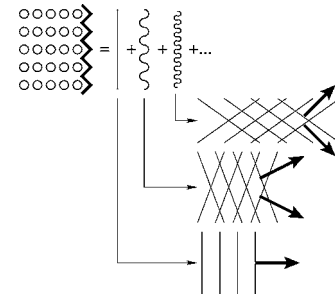
FIG. 7. Graphical illustration of mode matching: The triangular wave represents the field profile just inside the crystal. It has the periodicity of the lattice and must be matched to plane waves. The periodic profile is separated in a Fourier series, shown on the right. Each Fourier component corresponds to a superposition of plane waves in the homogeneous material shown at the bottom.

face, the well-known electromagnetic boundary conditions of continuity of tangential components of the electric and magnetic fields must hold. The superposition of modes on two sides of the interface must therefore have the same profile. In the photonic crystal, the fields are periodic with the periodicity of the lattice, as required by the Bloch theorem. This means that the superposition of waves on the other side of the interface must have the same periodicity. Therefore, fields in the plane of the interface may be decomposed in a two-dimensional spatial Fourier series. The fields must be matched for each spatial Fourier frequency independently, as shown in Fig. 7.

In order to provide the necessary information for mode matching, the band-structure concept must be extended to include details of the decaying stop band modes in crystals. The normal band structure provides extensive information about the propagating Bloch modes, but it does not describe decaying modes. In many photonic crystal-based devices, such as resonators or waveguides, the stop band properties of the crystal are more important than the pass bands, since they determine how light is confined and how rapid the decay is. The band structure can be augmented to include decaying modes, with complex propagation vectors. The imaginary part of these vectors gives the decay constant. The band structure including both propagating and decaying bands is referred to as the complex band structure of a crystal. It will be used in this section in order to obtain results valid both inside and outside photonic stop bands. Several methods exist to calculate the complex band structure. The plane-wave-expansion method (Ho *et al.*, 1990) can be used directly by providing a complex propagation vector, and trying to obtain a real frequency eigenvalue (Suzuki and Yu, 1995). This, however, leads to an extensive search since, in general, complex propagation vectors lead to complex eigenvalues. A method based on the KKR method and scattering matrices has been demonstrated for photonic crystals composed of spherical scatterers (Stefanou *et al.*, 1992, 1998). Complex propagation vectors can also be obtained from

band-structure calculations using transfer or scattering matrices (Li and Lin, 2003), as will be reviewed in the next section, or through a modification of the PWEM, described in the next paragraphs.

The PWEM must be modified to express propagation vectors as eigenvalues, for given frequency inputs (Istrate *et al.*, 2005). Decaying Bloch modes are of importance only near interfaces, since they decay to zero in bulk crystals. Hence, only the component of the Bloch wave vector perpendicular to the interface should be complex. The wave vector is decomposed, therefore, into components perpendicular and parallel to the interface. Assuming that the interface is perpendicular to the $\hat{z}$ direction, this can be written as $\mathbf{k} = \mathbf{k}_\parallel + \hat{z} k_\perp$.

For simplicity of notation, the following summary will assume a two-dimensional photonic crystal of cylinders with the electric field polarized along the cylinder axis. The same derivation can be applied to other polarizations or three-dimensional crystals. In the two-dimensional case, the eigenvalue equation for the PWEM can be rewritten as (Busch and John, 1998)

$$\sum_{\mathbf{G}} \eta_{\mathbf{G}-\mathbf{G}'} |\mathbf{k}+\mathbf{G}|^2 A_{\mathbf{G}}^{\mathbf{k}} = \frac{\omega^2}{c^2} A_{\mathbf{G}'}^{\mathbf{k}}, \tag{29}$$

where $\mathbf{G}$ are the reciprocal-lattice vectors, $\eta_{\mathbf{G}-\mathbf{G}'}$ represents the Fourier expansion of the inverse of the dielectric constant, $\mathbf{k}$ is the wave vector of the mode, and $A_{\mathbf{G}}^{\mathbf{k}}$ is the plane-wave expansion of the mode: $E(\mathbf{r}) = \sum_{\mathbf{G}} A_{\mathbf{G}}^{\mathbf{k}} e^{i(\mathbf{k}+\mathbf{G})\cdot\mathbf{r}}$. ω is the unknown frequency eigenvalue. Equation (29) can be rewritten in matrix form as

$$\mathbf{PA} = \frac{\omega^2}{c^2} \mathbf{A}, \tag{30}$$

with the column vector $\mathbf{A}$ containing the plane-wave amplitudes $A_{\mathbf{G}}^{\mathbf{k}}$. Matrix $\mathbf{P}$ contains terms with powers of $k_\perp$ up to second order. These terms can be isolated and Eq. (30) rewritten (Istrate *et al.*, 2005) using a method first published for semiconductor heterostructures (Smith and Mailhiot, 1990),

$$k_\perp^2 \mathbf{M}_a \mathbf{A} + k_\perp \mathbf{M}_b \mathbf{A} + \mathbf{M}_c(\omega) \mathbf{A} = 0, \tag{31}$$

Equation (31) can then be manipulated to obtain an eigenvalue equation for $k_\perp$, which can be written in block form as

$$\begin{bmatrix} 0 & \mathbf{I} \\ -\mathbf{M}_a^{-1}\mathbf{M}_c(\omega) & -\mathbf{M}_a^{-1}\mathbf{M}_b \end{bmatrix} \begin{pmatrix} \mathbf{A} \\ k_\perp \mathbf{A} \end{pmatrix} = k_\perp \begin{pmatrix} \mathbf{A} \\ k_\perp \mathbf{A} \end{pmatrix}. \tag{32}$$

Equation (32) provides both the real and imaginary parts of the band structure along with the corresponding propagating or decaying Bloch modes. It has the further advantage that the frequency is the input, simplifying calculations for devices where the input frequency is known. It should be noted that decaying solutions also appear outside the photonic crystal pass bands. These solutions represent surface modes.

Other similar methods have been published for isotropic (Hsue and Yang, 2004) and anisotropic (Hsue *et al.*, 2005) materials. It should be noted that the imaginary dispersion relation near the band edge can also be approximated using an analytic continuation of the real dispersion (Kohn, 1959).

With knowledge of the complex band structure and Bloch modes, the diffraction coefficients can be found by enforcing boundary conditions between the photonic crystal modes and plane waves in the homogeneous region. These conditions are the continuity of the tangential electric field, along with its first derivative, at the interface. Since at the interface photonic crystal modes have the periodicity of the lattice, these fields are decomposed in a spatial Fourier series, with the boundary conditions enforced between each Fourier order and its corresponding diffraction order in the homogeneous material. Not all diffraction orders will be propagating waves. Most higher orders will be evanescent, confined near the interface. In the same way, most Bloch modes excited at the interface will be decaying; only a few, if any, will be propagating. The modes decaying in both directions from the interface serve to adapt the modes of the infinite crystals to the interface.

With the interface perpendicular to the z direction and the assumption that one wave is incident on the interface from the homogeneous material, superpositions of plane waves in this material can be written as

$$E(\mathbf{r}) = E_0^+ e^{i\mathbf{k}_0^+\cdot\mathbf{r}} + \sum_m E_m^- e^{i\mathbf{k}_m^-\cdot\mathbf{r}}. \tag{33}$$

Here the superscripts + and − represent wave propagating toward the interface and away from it, respectively. m counts the diffraction orders. All propagation vector components along the interface are related by reciprocal-lattice vectors of the periodic surface,

$$\mathbf{k}_{m,\parallel}^- = \mathbf{k}_{0,\parallel}^+ + \mathbf{G}_{m,\parallel}. \tag{34}$$

In the photonic crystal, the modes are denoted by $E_j^C(\mathbf{r})$. The spatial Fourier components of these modes in the plane of the interface are denoted by $E_{j,m}^C$, where m counts the Fourier orders. At the interface, the usual conditions of continuity of the electric field and its derivative must be enforced for each Fourier component separately,

$$E_m^+ + E_m^- = \sum_j C_j E_{j,m}^C, \tag{35}$$

$$k_{m,\perp}(E_m^+ - E_m^-) = \sum_j C_j F_{j,m}^C, \tag{36}$$

with $E_m^+ = E_0^+$ if $m=0$ and $E_m^+=0$ otherwise. $F_{j,m}^C$ is the z derivative of the mth Fourier component of crystal mode j, taken in the plane of the interface. The above equations can be solved for the unknown amplitudes E_m^- and C_j, which represent the reflection, transmission, and diffraction coefficients.

From these diffraction coefficients, the most important value is the specular reflection coefficient. It is real for reflection outside the stop band, but becomes complex with unit magnitude inside the stop band. As an
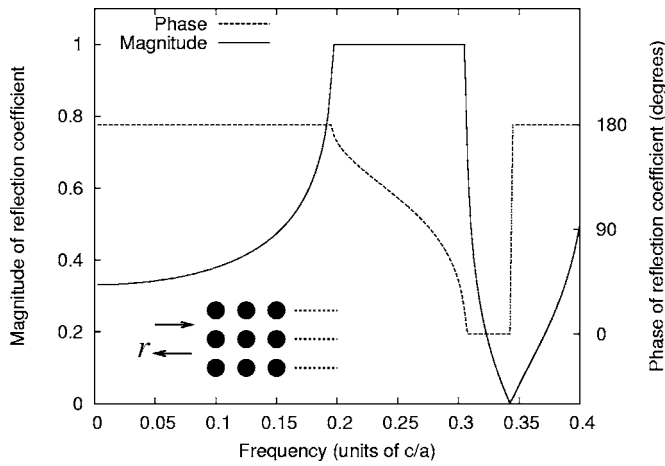
FIG. 8. Magnitude and phase of the reflection coefficient from a semi-infinite photonic crystal. The inset shows the geometry considered.

example, the reflection coefficient from a semi-infinite two-dimensional square photonic crystal of silicon cylinders in air is shown in Fig. 8. The cylinders have a radius of 0.3 lattice constant. The electric field is polarized along the cylinders.

The interface conditions for surfaces that do not correspond to Miller indices, as well as for input waves that are not plane waves, have also been calculated (Jiang *et al.*, 2005). For Gaussian input beams, the equifrequency surface of the crystal dispersion relation, which is responsible for the direction of propagation in the crystal, can be approximated as a quadratic function (Momeni and Adibi, 2003). This allows one to calculate an effective refractive index that can be used to compute the angle of propagation of light entering a crystal with the usual Snell equation.

The magnitude of reflection coefficients has been measured by many groups. The reflection phase has also been measured in a few cases. At microwave frequencies it was measured directly using a network analyzer (Özbay and Temelkuran, 1996). At optical frequencies it was measured for a three-dimensional colloidal crystal using resonance frequencies of a large Fabry-Perot resonator (Istrate *et al.*, 2005a). For a two-dimensional photonic crystal, the standing waves in front of the crystal have been measured using coupling of the evanescent tail of the mode into a tapered fiber (Flück *et al.*, 2003).

3. Transmission and reflection coefficients calculated with transfer matrices

An alternative method to calculate the response of semi-infinite photonic crystals is through the use of scattering or transfer matrices (Li and Ho, 2003), using a reciprocal-space representation of the crystal in directions parallel to the interface, and a real-space representation perpendicular to the interface. As before, the first step is to calculate the band structure of the crystal. It is convenient to obtain this from the scattering matrix (Li and Lin, 2003). The structure is separated into thin slices parallel to the interface plane. It is assumed that all

slices are separated by infinitesimally thin air regions. This allows fields in the air regions to be expressed in a plane-wave basis, the same basis as is used outside the crystal. As they do not have any width, these air regions will not affect the electromagnetic modes.

Assuming again for simplicity a two-dimensional photonic crystal with the electric field polarized along the cylinders and the interface parallel to the $\hat{z}$ direction, the electric field in the air regions is expanded as

$$E(\mathbf{r}) = \sum_m \left[E_m^+(z) + E_m^-(z)\right]e^{i\mathbf{k}_{m,\parallel} \cdot \mathbf{r}_\parallel}, \quad (37)$$

where m counts again the diffraction orders, the + and − superscripts denote the waves propagating to the right and the left, respectively, the $\parallel$ subscript denotes components in the plane parallel to the interface, and $\mathbf{k}_m$ differs from the incident wave vector $\mathbf{k}_0$ by a reciprocal-lattice vector of the periodic slice: $\mathbf{k}_m = \mathbf{k}_0 + \mathbf{G}_m$.

The amplitudes of the plane waves in each air region, E_m^+ and E_m^-, are written as column vectors $\mathbf{\Omega}_i^+$ and $\mathbf{\Omega}_i^-$. The subscript i counts slices in the crystal. Transfer matrices are then computed to relate electric fields in adjacent slices, assuming that these slices are thin enough to be approximated as constant in the $\hat{z}$ direction,

$$\begin{pmatrix} \mathbf{\Omega}_i^+ \\ \mathbf{\Omega}_i^- \end{pmatrix} = \mathbf{T}_i \begin{pmatrix} \mathbf{\Omega}_{i-1}^+ \\ \mathbf{\Omega}_{i-1}^- \end{pmatrix}, \quad (38)$$

where $\mathbf{T}_i$ is the transfer matrix for slice i.

In order to obtain the band structure of the crystal, the transfer matrix for a whole unit cell must be obtained by multiplying the transfer matrices for all slices inside the unit cell. Calling this matrix $\mathbf{T}$, it can be inserted into the Bloch equation,

$$\mathbf{T} \begin{pmatrix} \mathbf{\Omega}_0^+ \\ \mathbf{\Omega}_0^- \end{pmatrix} = e^{i\mathbf{k} \cdot \mathbf{a}_3} \begin{pmatrix} \mathbf{\Omega}_0^+ \\ \mathbf{\Omega}_0^- \end{pmatrix}, \quad (39)$$

where $\mathbf{k}$ is the Bloch propagation vector of the crystal, whose components $\mathbf{k}_\parallel$ have been used to set up the plane-wave basis. $\mathbf{a}_3$ is the lattice vector that does not lie in the plane of the interface. Equation (39) forms an eigenvalue equation for the unknown propagation vector perpendicular to the interface, given the frequency and propagation vector components parallel to the interface.

The transfer matrix method described above suffers from instability, due to growing exponential functions. This can be avoided by working with scattering matrices, instead of transfer matrices, which provide the following relations:

$$\begin{pmatrix} \mathbf{\Omega}_i^+ \\ \mathbf{\Omega}_{i-1}^- \end{pmatrix} = \mathbf{S}_i \begin{pmatrix} \mathbf{\Omega}_{i-1}^+ \\ \mathbf{\Omega}_i^- \end{pmatrix}. \quad (40)$$

Scattering matrices for adjacent slices can be combined using a recursive algorithm (Li, 1996; Pendry, 1996) to yield a scattering matrix for an entire unit cell. Using the Bloch theorem again, the band structure can be computed using the following generalized eigenvalue equation:

$$\begin{pmatrix} \mathbf{S}_{11} & 0 \\ \mathbf{S}_{21} & -\mathbf{I} \end{pmatrix}\begin{pmatrix} \mathbf{\Omega}_0^+ \\ \mathbf{\Omega}_0^- \end{pmatrix} = e^{i\mathbf{k}\cdot\mathbf{a}_3}\begin{pmatrix} \mathbf{I} & -\mathbf{S}_{12} \\ 0 & -\mathbf{S}_{22} \end{pmatrix}\begin{pmatrix} \mathbf{\Omega}_0^+ \\ \mathbf{\Omega}_0^- \end{pmatrix}. \quad (41)$$

The transfer matrices computed above relate the electric fields in neighboring unit cells, keeping track of which waves are traveling to the right and which to the left. It is therefore possible to compute the response of a semi-infinite crystal by considering a single unit cell of a crystal, setting the wave that enters the crystal from the far end to zero. This is done (Li and Ho, 2003) by first finding a matrix $\mathbf{D}$ that diagonalizes the transfer matrix for a unit cell: $\mathbf{T}=\mathbf{D}\mathbf{\Lambda}\mathbf{D}^{-1}$, where $\mathbf{\Lambda}$ is the diagonal matrix containing eigenvalues of the transfer matrix. The eigenvalue equation can then be rewritten as

$$\mathbf{\Lambda}\mathbf{\Sigma}_0 = \lambda\mathbf{\Sigma}_0, \quad (42)$$

where $\lambda = e^{i\mathbf{k}\cdot\mathbf{a}_3}$ is the eigenvalue of the transfer matrix. $\mathbf{\Sigma}_i$ is defined as

$$\mathbf{\Sigma}_i = \begin{pmatrix} \mathbf{\Sigma}_i^+ \\ \mathbf{\Sigma}_i^- \end{pmatrix} = \mathbf{D}^{-1}\begin{pmatrix} \mathbf{\Omega}_i^+ \\ \mathbf{\Omega}_i^- \end{pmatrix}. \quad (43)$$

Since $\mathbf{\Lambda}$ is diagonal, the vector $\mathbf{\Sigma}$ after propagation through n unit cells can be written as

$$\begin{pmatrix} \mathbf{\Sigma}_n^+ \\ \mathbf{\Sigma}_n^- \end{pmatrix} = \mathbf{\Lambda}^n\mathbf{\Sigma}_0 = \begin{pmatrix} \mathbf{\Lambda}_+^n & 0 \\ 0 & \mathbf{\Lambda}_-^n \end{pmatrix}\begin{pmatrix} \mathbf{\Sigma}_0^+ \\ \mathbf{\Sigma}_0^- \end{pmatrix}. \quad (44)$$

If the crystal is semi-infinite, there will be no reflection from its back facet. Hence, there will be no modes propagating toward the front of the crystal, resulting in $\mathbf{\Sigma}_0^-=0$. This condition produces the following relations for electric fields in front of the structure:

$$\mathbf{\Omega}_0^+ = \mathbf{D}_{11}\mathbf{\Sigma}_0^+, \quad (45)$$

$$\mathbf{\Omega}_0^- = \mathbf{D}_{21}\mathbf{\Sigma}_0^+. \quad (46)$$

The reflection of light from the crystal can then be written as

$$\mathbf{\Omega}_0^- = \mathbf{D}_{21}\mathbf{D}_{11}^{-1}\mathbf{\Omega}_0^+ \quad (47)$$

and a similar expression can be obtained for transmittance into the crystal.

Instead of explicitly setting the reflection from the back facet to zero, as was described above, this reflection can also be eliminated by including a small amount of loss (Botten et al., 2001). A similar method was also derived for photonic crystals composed of a periodic array of metallic disks (Contopanagos et al., 1999), using the impedance of each lattice plane. The derivation, however, did not include the effects of diffraction into multiple plane waves. For opal photonic crystals, the reflection has also been estimated from overlap integrals with bulk modes (Ochiai and Sánchez-Dehesa, 2001).

The preceding two subsections have described two different methods to compute reflection and transmission coefficients at photonic crystal boundaries, one based on the Bloch modes of the infinite crystals and one based on transfer matrices. These two methods can be combined to extract the efficiency of the PWEM

when dealing with large, perfectly periodic areas, while allowing arbitrary defects (Green et al., 2005).

4. Device analysis using effective medium boundary conditions

The methods presented in the previous section allow homogenization of photonic crystals, replacing each periodic section by an effective medium, characterized by boundary conditions at the interfaces and by their dispersion relations between the interfaces. Now photonic crystal devices can be interpreted as a succession of effective materials, some periodic and some homogeneous.

Calculation of the response of dielectric devices with few interfaces is done by assuming propagation in plane waves in each material, connected by the well-known boundary conditions at the interfaces. This approach is now possible with photonic crystal devices as well.

The simplest case to consider is that of light traversing a photonic crystal slice of finite size (Istrate et al., 2005). The well-known Airy formula developed for thin dielectric slabs can be applied directly, since the reflection coefficients are known,

$$r = r_{12} + \frac{t_{12}t_{21}r_{23}e^{2i\phi}}{1 - r_{21}r_{23}e^{2i\phi}}, \quad (48)$$

where r_{ij} represents the reflection coefficient at the interface from material i to j and $\phi=k_\perp L$ is the phase change of the wave across the photonic crystal, calculated from the photonic crystal dispersion relation. r is the reflection from the slab. Since Eq. (48) takes into account multiple reflections from the two facets, it represents correctly the resonant transmittance fringes and other surface effects that were observed previously (Sakoda, 1995a).

For localized light sources, a similar calculation was performed (Yang et al., 2005) where the input fields are first decomposed into Fourier components. The transfer matrix method from the previous section was also used to compute the states of photonic crystal quantum wells (Feng et al., 2005), again taking into account multiple reflections inside the cavity.

The resonant states of point-defect cavities are calculated in an equally intuitive fashion, starting from the requirement that the wave interfere resonantly with itself after one round-trip through the cavity. For a defect in a square photonic crystal, the round-trip condition must be enforced in two orthogonal directions at once. Inside the defect, light propagates as a superposition of plane waves. These plane waves must all undergo a phase change of a multiple of 2π after a round trip. For the two directions this can be written as

$$k_x L_x + \phi_x(k_z,\omega) = l\pi,$$

$$k_z L_z + \phi_z(k_x,\omega) = m\pi, \quad (49)$$

where l and m are integers. k_x and k_z are components of the propagation vectors in the cavity. They are related by the energy conservation requirement $k_x^2+k_z^2=k^2$

$=(n\omega/c)^2$. L_x and L_z are the dimensions of the cavity in the two directions, and ϕ_x and ϕ_z are the phase shifts encountered upon reflection from the photonic crystal interfaces. $\phi_x(k_z,\omega)$ is the phase change upon reflection from an interface parallel to the z direction. It depends on frequency and also on the angle of the incoming wave. This incident angle is determined by k_z. In the same manner, ϕ_z describes reflections at interfaces parallel to the x direction and depends on k_x and ω.

The same conditions of constructive interference after one round trip can also be used for the design of photonic crystal waveguides (Istrate and Sargent, 2005b). Using a ray-optics picture, light travels along the guide by reflecting off two claddings. Since the cladding interfaces are periodic, they may also diffract waves. The mode condition can be found by insisting that all diffracted waves return after one round trip across the waveguide with the same amplitude and phase relations.

In most practical devices, when waves diffract at the periodic interfaces, up to three propagating diffraction orders can appear. The rest will be evanescent with a decay strong enough so that they will not be able to carry any significant optical power from one cladding interface to the other one. These evanescent diffraction orders are therefore ignored. The derivation shown here assumes that three propagating diffraction orders are indeed present. The equations can be simplified easily if there are fewer orders.

The various plane waves in the core of the waveguide are denoted by the complex amplitudes E_1, E_2, and E_3 measured at a point just before they reach the cladding interface. At the interface they will diffract into each other, as given by the complex diffraction coefficients d_{ij} described in Sec. V.F.2 denoting diffraction from plane wave i to j. After diffraction at the interface and propagation to the opposite cladding, the complex amplitudes of the fields will be denoted by E_1', E_2', and E_3'. The two sets of amplitudes are related by

$$E_1' = (E_1 d_{11} + E_2 d_{21} + E_3 d_{31})e^{ik_{x1}L},$$

$$E_2' = (E_1 d_{12} + E_2 d_{22} + E_3 d_{32})e^{ik_{x2}L}, \qquad (50)$$

$$E_3' = (E_1 d_{13} + E_2 d_{23} + E_3 d_{33})e^{ik_{x3}L}.$$

The above set of equations can be written in matrix form by using vectors $\mathbf{E}$ and $\mathbf{E}'$ to contain the fields E_i and E_i', respectively, and the matrix $\mathbf{M}$ to relate the two,

$$\mathbf{E}' = \mathbf{M}\mathbf{E}. \qquad (51)$$

The matrix $\mathbf{M}$ essentially describes propagation through half of a round trip. A similar matrix $\mathbf{N}$ can be set up to complete the round trip, relating the fields $\mathbf{E}'$ at the second interface to the fields $\mathbf{E}''$ at the first interface. The mode condition then requires that $\mathbf{E}''=\mathbf{E}$,

$$\mathbf{E}'' = \mathbf{N}\mathbf{M}\mathbf{E} = \mathbf{E}, \qquad (52)$$

which means that the matrix $\mathbf{N}\mathbf{M}$ must have an eigenvalue equal to 1. For symmetric waveguides, whose modes can be divided into symmetric and antisymmetric

classes, matrices $\mathbf{M}$ and $\mathbf{N}$ will be equal. The mode condition in this case can be simplified by requiring that matrix $\mathbf{M}$ have an eigenvalue equal to ±1.

In a similar way, the response of photonic crystal waveguide couplers can be computed using diffraction coefficients to calculate the even and odd supermodes of the couplers, from which the coupling lengths and coupling constants are easily obtained. The coupling constant can then be used to calculate the coupling from a photonic crystal waveguide to a point defect lying next to the guide.

As was seen here, the devices are separated into sections of effective materials connected by boundary conditions. Similar structures involving uniform dielectrics have been solved using transfer or scattering matrices, assigning one matrix to each interface and one to each uniform section. The same matrix formalism can also be applied to the photonic crystal interfaces described here (Istrate and Sargent, 2005b) to provide a systematic way of writing the necessary equations for structures with multiple interfaces.

The above examples have used interfaces between photonic crystals and homogeneous materials. The same techniques can be used for heterostructure devices. As mentioned above, such a heterostructure can be described by a three-layer structure with two photonic crystals separated by an infinitely thin homogeneous layer. As the thickness of the center layer vanishes, the resulting transmission, reflection, and diffraction tend to the correct values for the heterostructure. One problem encountered in this case is that two crystals may have different lattice constants, resulting in different propagation vectors for the various diffraction orders. This means that the Fourier decomposition of the field profiles in the interface plane will have different components. A possible solution is to perform the decomposition on a larger section of the interface, corresponding to an integer number of lattice constants in each crystal (Feng et al., 2005).

The boundary conditions described here replace uniform photonic crystal sections with effective materials, assuming that the modes of the infinite materials are a good representation of the finite crystals. If these crystal sections become very thin, however, the assumption will introduce errors. This usually happens for crystals less than four layers thick. For such thin crystals, a better solution is to combine the reflection and diffraction coefficients in larger crystals with a scattering matrix representation in the thin crystals (Green et al., 2005). This preserves both generality and efficiency.

The above interface properties and associated transfer matrices have been calculated for simple planar interfaces. Similar matrices can also be computed for much more complex structures, such as entire sections of waveguides and waveguide bends (Mingaleev and Busch, 2003). This allows complex optical circuits to be assembled from a set of building blocks, such as various types of bent and straight waveguide sections and other optical elements. The response of the entire system can

then be computed easily, if the responses of the individual sections are known.

G. Defect analysis and design based on symmetry and momentum considerations

The goal of the preceding sections has been to provide simplified methods to solve the wave equations in photonic crystals with deviations from perfect periodicity. It is possible, however, to obtain significant information about resonant cavities and defects from considerations of the crystal and defect symmetries. One particular area where this information is of value is in the design of two-dimensional crystal devices that minimize out-of-plane radiation.

For one-dimensional photonic crystals with a weak modulation in refractive index, the Bloch modes may be approximated by sinusoids arranged according to the well-known requirement that the electric field is concentrated in the high-dielectric regions at the lower band edges and in the low-dielectric regions at the upper edges (Joannopoulos *et al.*, 1995). Even when the dielectric modulation increases, many of the qualitative properties of this simple model still hold. Such an approximate representation of the modes is also useful in crystals of higher dimensionality. The symmetries of the crystal, as given by space group theory, can be used to determine the shapes of photonic crystal modes (Sakoda, 1995b). The same group theory is then used to classify resonant modes in photonic crystal defects, resulting in a set of allowed mode profiles in the defects (Painter and Srinivasan, 2003) based on the symmetry of the defect.

The symmetry properties of the resonant states are well suited to the investigation and reduction of radiation losses from two-dimensional photonic crystal resonators fabricated in slab waveguides. The bulk Bloch modes in such crystals can be divided in two classes: those above and below the light cone. The ones above have a small enough in-plane wave vector to be able to couple to radiating modes above the slab. Those below have a wave vector larger than what is possible for propagating modes outside the slab. These modes are therefore well confined to the slab in the absence of fabrication imperfections. A similar effect is also seen with photonic crystal waveguides fabricated in semiconductor slabs. Guided modes with propagation constants larger than what is possible outside the slabs will not radiate (Johnson *et al.*, 1999), with the mode being confined to the slab by index guiding.

For photonic crystal resonators fabricated in two-dimensional crystals, however, it is impossible to completely eliminate radiation. Since the optical mode is confined to the neighborhood of the defect, it has a limited spatial extent. Its profile, expressed in two-dimensional spatial Fourier space, will have Fourier components small enough to fall in the radiating region. While it is not possible to completely eliminate this radiation, it can be reduced to negligible levels. One of the first methods that was introduced to reduce radiation

losses required that radiated fields cancel in the far field leading to a set of nulls in the far-field pattern (Johnson *et al.*, 2001). This was obtained by a cavity mode with odd symmetry, making sure that the spatial Fourier components near zero vanish. Optimizing a cavity using this approach led to a quality factor of approximately 30 000.

Even when using odd modes in the cavities, the momentum distribution of the modes can be further optimized to push most of the mode energy to momentum values that fall outside the light cone (Srinivasan and Painter, 2002, 2003). Symmetry considerations are used to select the best unoptimized mode. This will, for example, indicate whether the best starting point is a defect of increased or reduced dielectric constant, and also the best position for the center of the mode. Further optimizations are then performed to distribute the momentum components in the most favorable way while still maintaining good confinement in the plane of the slab. The best structures for this purpose have been found to be graded photonic crystals, with a gradual increase in the strength of the stop band away from the center of the defect (Srinivasan and Painter, 2002), as well as abrupt heterostructures.

Engineering the Fourier components of the defect modes has been used for a number of record-breaking quality factor measurements. In a graded photonic crystal defect, the quality factor Q was measured to be 40 000 (Srinivasan, Barclay, *et al.*, 2004). Optimizing the positions of the cylinders in the neighborhood of a point defect led to a cavity with $Q = 45\,000$ (Akahane *et al.*, 2003). Using heterostructure cavities for the same purpose produced $Q = 600\,000$ (Song, Noda, *et al.*, 2005).

H. Analysis methods for semiconductor devices

Many of the techniques presented earlier have been derived from developments in semiconductor heterostructures. This subsection gives a brief review of the analysis methods for equivalent electronic devices.

Due to the crystalline periodicity, electrons in semiconductors exist in Bloch states. These states are composed of a traveling-wave component modulated by a periodic function. The relationship between the wave vector of the traveling-wave component and energy is given by the semiconductor dispersion relation. Since in most semiconductors this dispersion relation is parabolic near the band extrema, similar to the dispersion of free space, one can approximate the movement of an electron in this material with movement in free space, but with a different mass, called the effective mass.

The effective mass depends on the semiconductor material and band. It includes all of the necessary crystal properties in order to describe the electron motion as a particle propagating through a region of constant potential, when in fact the electron feels the periodic attraction of all atoms. The effective mass makes it possible to employ many equations from classical mechanics, such as Newton's law of motion, to calculate the acceleration of an electron. By collecting the salient properties of the semiconductor into a small number of parameters—the

energetic locations of the band extrema and effective masses—many devices can be understood very easily, usually with sufficient numerical precision.

In most cases the parabolic band approximation—required by the effective mass—is valid, especially near the band edges where the highest charge-carrier concentrations are found. Far from the edges, however, the bands deviate significantly from a parabola reducing the validity of such approximations.

The effective masses can be measured using cyclotron resonance experiments (Dresselhaus *et al.*, 1955). The results are tabulated for most semiconductors for both the conduction and valence bands. They can, however, also be computed from the curvature of the dispersion relation. An easier method, however, is given by the $k \cdot p$ analysis (Bastard, 1988), where the effective mass is computed from the Bloch modes instead of the band curvature. Further improvements to the band curvature approximations are given by the Kane (1957) model.

Semiconductor heterojunctions involve two or more semiconductors which form a single crystal. The potential energy experienced by electrons in such structures is a superposition of the periodic potential due to the crystals and the potential steps representing the differences in band energies across the junction. It is impractical to consider the potential of all atoms when calculating the properties of the structure. The envelope approximation (Sai-Halasz *et al.*, 1977; Bastard, 1981) is used to address this issue.

As was done with bulk semiconductors, the periodic potential profile of each crystal can be replaced by a material parameter, which is again the effective mass. With this approximation, the only varying potential left in the problem is that of the heterojunction. In most practical cases the number of heterointerfaces is quite small leading to simple quantum-mechanical problems, as illustrated in Fig. 9.

When using this approximation, only the envelope of the atomic potential energy is used. All other properties of the semiconductors are hidden in the effective mass. As a result, one does not obtain the exact wave function of the electron in the heterojunction, but only its envelope. The envelope is usually sufficient to find confinement of electrons, resonant frequencies, and most other parameters of practical interest for an electronic device.

While the envelope approximation can be used effectively to compute electronic states in semiconductor heterostructures, the wave function at the heterojunction, the plane where the two semiconductors meet, is not described well. In usual quantum structures, simple boundary conditions of continuity of the wave function and its derivative at an interface are imposed. This is, however, no longer the case when using the envelope approximation, since the envelope obeys its own equation instead of the Schrödinger equation. While the envelope of the wave function must remain continuous, its first derivative does not. Several boundary conditions have been proposed (Zhu and Kroemer, 1983; Galbraith and Duggan, 1988; Grinberg and Luryi, 1989; Foreman, 1998) over the past three decades, each valid for differ-
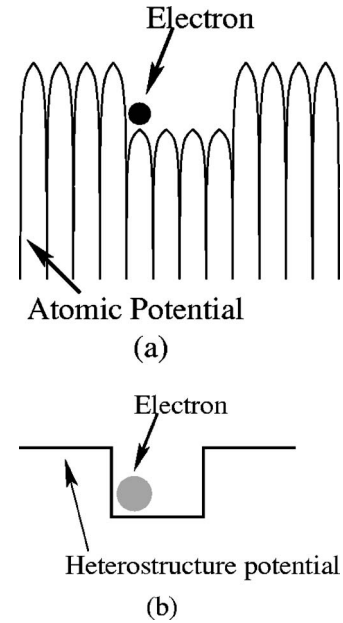
FIG. 9. The use of the envelope approximation and effective mass in semiconductor structures. (a) True atomic potential. (b) Heterostructure potential and effective mass.

ent semiconductors, and in different situations.

Envelope function approximations express the heterostructure modes as superpositions of the bulk modes, modulated by slowly varying envelopes. In particular, decaying wave functions in a semiconductor band gap are expressed as superpositions of traveling solutions, modulated by a decaying envelope. An alternative method has been described that uses the true semiconductor Bloch modes at every point in the heterostructure (Smith and Mailhiot, 1990). In the first step of the method, eigenstates of the bulk material Hamiltonian are found in each semiconductor. Since the electron energy (ω) and propagation vector parallel to the interface ($\mathbf{k}_\parallel$) are conserved across the interface, eigenstates are calculated with ω and $\mathbf{k}_\parallel$ as inputs. This will result in a set of Bloch modes which in general have a complex propagation vector perpendicular to the interface ($k_\perp$). Eigenstates with real $k_\perp$ correspond to propagating modes, while complex values represent decaying modes which have significant amplitude only near the interface. This is the case for all modes in the band gap, but also appears for energies outside the gap. The imaginary part of $k_\perp$ describes the decay length in the crystal (Smith and Mailhiot, 1986).

The complex eigenmodes of two crystals, with equal ω and $\mathbf{k}_\parallel$, are then matched at the interface (Aversa and Sipe, 1993). The condition to be enforced there is the continuity of electron flux (Bastard, 1988). For a given set of waves incident on the interface, the corresponding set of outgoing waves is obtained. The most significant difference between this approach and the envelope approximation is that the amplitudes of the bulk Bloch modes are constant. Decay in the stop band is described by decaying Bloch modes. As a result, there is no enve-

lope equation to be solved at each point in the hetero-structure.

The use of the $k \cdot p$ approach described above is based on the nearly free electron model for semiconductors, where the crystal lattice is assumed to form a small perturbation from free space. A complementary approach has also been taken in the tight-binding method. Here the electronic wave functions are assumed to be very similar to those of independent atoms. The effects of neighboring atoms are treated as perturbations (Ashcroft and Mermin, 1976). Using this method, electron states are represented in a basis of functions that are highly localized at the lattice sites.

Both the effective mass and tight-binding approximations have been applied to photonic crystal devices. Effective masses are useful for devices with large periodic sections, such as heterostructure waveguides. In contrast, tight-binding approaches are most efficient for devices with defect modes of small extent, such as those produced by point-defect resonators and line-defect waveguides.

VI. CONCLUSIONS

Semiconductor heterostructures have revolutionized optoelectronics and high-speed electronics through their ability to confine electrons of precise kinetic energies in specific device areas. Photonic crystal heterostructures provide a similar amount of control over the wavelength and localization of light in photonic crystals. For this reason they have become an important building block for photonic crystal devices. While the initial device proposals were based on point and line defects, some of the best-performing waveguides and resonators were fabricated using heterostructures including both abrupt and graded junctions.

The simulation of heterostructure devices is difficult with standard tools, due to the large device volumes that must be treated with great accuracy. The analogy between semiconductors and photonic crystals, however, has allowed the introduction of several highly optimized design and analysis methods derived from their solid-state counterparts.

While individual heterojunctions and simple devices have been demonstrated and reviewed here, improvements in the quality of fabricated heterostructures, especially using self-assembled colloidal crystals, will lead to more complex optical devices. Such heterostructures are expected to provide a means for the realization of multiple devices, integrated on a common platform, where active and passive functions are obtained by selective infiltration of the porous structures with different materials. This will lead to the necessary devices for more complex optical systems required in the future.

REFERENCES

Akahane, Y., T. Asano, B. S. Song, and S. Noda, 2003, "High-Q photonic nanocavity in a two-dimensional photonic crystal," Nature (London) **425**, 944–947.

Albert, J. P., C. Jouanin, D. Cassagne, and D. Bertho, 2000, "Generalized Wannier function for photonic crystals," Phys. Rev. B **61**, 4381–4384.

Albert, J. P., C. Juanin, D. Cassagne, and D. Monge, 2002, "Photonic crystal modelling using a tight-binding Wannier function method," Opt. Quantum Electron. **34**, 251–263.

Alferov, Z., 2000, "Double heterostructure lasers: Early days and future perspectives," IEEE J. Sel. Top. Quantum Electron. **6**, 832–840.

Anderson, P. W., 1958, "Absence of diffusion in certain random lattices," Phys. Rev. **109**, 1492–1505.

Ashcroft, N. W., and N. D. Mermin, 1976, *Solid State Physics* (Holt, Rinehart and Winston, New York).

Aversa, C., and J. E. Sipe, 1993, "Semiconductor-heterostructure-interface connection rules," Phys. Rev. B **47**, 6590–6597.

Baba, T., D. Mori, K. Inoshita, and Y. Kuroki, 2004, "Light localizations in photonic crystal line defect waveguides," IEEE J. Sel. Top. Quantum Electron. **10**, 484–491.

Barclay, P., K. Srinivasan, and O. Painter, 2003, "Design of photonic crystal waveguides for evanescent coupling to optical fiber tapers and integration with high-Q cavities," J. Opt. Soc. Am. B **20**, 2274–2284.

Bastard, G., 1981, "Superlattice band structure in the envelope-function approximation," Phys. Rev. B **24**, 5693–5697.

Bastard, G., 1988, *Wave Mechanics Applied to Semiconductor Heterostructures* (Les Éditions de Physique, Les Ulis, France).

Bell, P. M., J. B. Pendry, L. M. Moreno, and A. J. Ward, 1995, "A program for calculating photonic band structures and transmission coefficients of complex structures," Comput. Phys. Commun. **85**, 306–322.

Bhandari, R., 1990, in *Analogies in Optics and Micro Electronics*, edited by W. van Haeringen and D. Lenstra (Kluwer Academic, Dodrecht, The Netherlands), pp. 69–81.

Bhat, N. A. R., and J. E. Sipe, 2001, "Optical pulse propagation in nonlinear photonic crystals," Phys. Rev. E **64**, 056604.

Blanco, A., *et al.*, 2000, "Large-scale synthesis of a silicon photonic crystal with a complete three-dimensional bandgap near 1.5 micrometers," Nature (London) **405**, 437–440.

Botten, L. C., N. A. Nicorovici, R. C. McPhedran, C. M. de Sterke, and A. A. Asatryan, 2001, "Photonic band structure calculations using scattering matrices," Phys. Rev. E **64**, 046603.

Busch, K., and S. John, 1998, "Photonic band gap formation in certain self-organizing systems," Phys. Rev. E **58**, 3896–3908.

Busch, K., S. F. Mingaleev, A. Garcia-Martin, M. Schillinger, and D. Hermann, 2003, "The Wannier function approach to photonic crystal circuits," J. Phys.: Condens. Matter **15**, R1233–R1256.

Campbell, M., D. N. Sharp, M. T. Harrison, R. G. Denning, and A. J. Turberfield, 2000, "Fabrication of photonic crystals for the visible spectrum by holographic lithography," Nature (London) **404**, 53–56.

Capasso, F., 1992, "Bandgap and interface engineering for advanced electronic and photonic devices," Thin Solid Films **216**, 59–67.

Capasso, F., S. Sen, F. Beltram, L. M. Lunardi, A. S. Vengurlekar, P. R. Smith, N. J. Shah, R. J. Malik, and A. Y. Cho, 1989, "Quantum functional devices: Resonant-tunneling transistors, circuits with reduced complexity, and multiple-valued logic," IEEE Trans. Electron Devices **36**, 2065–2081.

Capasso, F., *et al.*, 2002, "Quantum cascade lasers: Ultrahigh-

speed operation, optical wireless communication, narrow linewidth, and far-infrared emission," IEEE J. Quantum Electron. **38**, 511–532.

Chan, C. T., Q. L. Yu, and K. M. Ho, 1995, "Order-N spectral method for electromagnetic waves," Phys. Rev. B **51**, 16635–16642.

Chang, L. L., L. Esaki, and R. Tsu, 1974, "Resonant tunneling in semiconductor double barriers," Appl. Phys. Lett. **24**, 593–595.

Charbonneau-Lefort, M., E. Istrate, M. Allard, J. Poon, and E. H. Sargent, 2002, "Photonic crystal heterostructures: Waveguiding phenomena and methods of solution in an envelope function picture," Phys. Rev. B **65**, 125318.

Chutinan, A., and S. John, 2004, "Diffractionless optical networking in an inverse opal photonic band gap micro-chip," Photonics Nanostruct. Fundam. Appl. **2**, 41–49.

Chutinan, A., S. John, and O. Toader, 2003, "Diffractionless flow of light in all-optical microchips," Phys. Rev. Lett. **90**, 123901.

Cohen-Tannoudji, C., B. Diu, and F. Laloë, 1977, *Quantum Mechanics* (Wiley, New York), Vol. 1.

Coldren, L., and S. W. Corzine, 1995, *Diode Lasers and Photonic Integrated Circuits* (Wiley, New York).

Contopanagos, H. F., C. A. Kyriazidou, W. M. Merrill, and N. G. Alexopoulos, 1999, "Effective response functions for photonic bandgap materials," J. Opt. Soc. Am. A **16**, 1682–1699.

Denkov, N. D., O. D. Velev, P. A. Kralchevsky, I. B. Ivanov, H. Yoshimura, and K. Nagayama, 1993, "Two-dimensional crystallization," Nature (London) **361**, 26.

de Sterke, C. M., and J. E. Sipe, 1988, "Envelope-function approach for the electrodynamics of nonlinear periodic structures," Phys. Rev. A **38**, 5149–5165.

Dimitrov, A. S., and K. Nagayama, 1996, "Continuous convective assembling of fine particles into two-dimensional arrays on solid surfaces," Langmuir **12**, 1303–1311.

Dresselhaus, G., A. F. Kip, and C. Kittel, 1955, "Cyclotron resonance of electrons and holes in silicon and germanium crystals," Phys. Rev. **98**, 368–384.

Eaves, L., 1990, in *Analogies in Optics and Micro Electronics*, edited by W. van Haeringen and D. Lenstra (Kluwer Academic, Dordrecht), pp. 227–242.

Egen, M., R. Voss, B. Griesebock, R. Zentel, S. Romanov, and C. S. Torres, 2003, "Heterostructures of polymer photonic crystal films," Chem. Mater. **15**, 3786–3792.

Elson, J. M., and P. Tran, 1995, "Dispersion in photonic media and diffraction from gratings: A different modal expansion for the R-matrix propagation technique," J. Opt. Soc. Am. A **12**, 1765–1771.

Elson, J. M., and P. Tran, 1996, "Coupled-mode calculation with the R-matrix propagator for the dispersion of surface waves on a truncated photonic crystal," Phys. Rev. B **54**, 1711–1715.

Esaki, L., 1986, "A bird's-eye view on the evolution of semiconductor superlattices and quantum wells," IEEE J. Quantum Electron. **22**, 1611–1624.

Feldmann, J., K. Leo, J. Shah, D. A. B. Miller, and J. E. Cunningham, 1992, "Optical investigation of Bloch oscillations in a semiconductor superlattice," Phys. Rev. B **46**, 7252–7255.

Feng, C. S., L. M. Mei, L. Z. Cai, P. Li, and X. L. Yang, 2005, "Resonant modes in quantum well structure of photonic crystals with different lattice constants," Solid State Commun. **135**, 330–334.

Flück, E., M. Hammer, A. M. Otter, J. P. Korterik, L. Kuipers,

and N. F. van Hulst, 2003, "Amplitude and phase evolution of optical fields inside periodic photonic structures," J. Lightwave Technol. **21**, 1384–1392.

Foreman, B. A., 1998, "Connection rules versus differential equations for envelope functions in abrupt heterostructures," Phys. Rev. Lett. **80**, 3823–3826.

Fritzsche, D., 1987, "Heterostructures in MODFETs," Solid-State Electron. **30**, 1183–1195.

Galbraith, I., and G. Duggan, 1988, "Envelope-function matching conditions for GaAs/(Al,Ga)As heterojunctions," Phys. Rev. B **38**, 10057–10059.

Galisteo-Lopez, J., F. Garcia-Santamaria, D. Golmayo, B. Juarez, C. Lopez, and E. Palacios-Lidon, 2004, "Design of photonic bands for opal-based photonic crystals," Photonics Nanostruct. Fundam. Appl. **2**, 117–125.

Gaponik, N., A. Eychmüller, A. L. Rogach, V. G. Solovyev, C. M. S. Torres, and S. G. Romanov, 2004, "Structure-related optical properties of luminescent hetero-opals," J. Appl. Phys. **95**, 1029–1035.

Gaylord, T. K., G. N. Henderson, and E. N. Glytsis, 1993, "Application of electromagnetics formalism to quantum-mechanical electron-wave propagation in semiconductors," J. Opt. Soc. Am. B **10**, 333–339.

Green, A. A., E. Istrate, and E. H. Sargent, 2005, "Efficient design and optimization of photonic crystal waveguides and couplers: The interface diffraction method," Opt. Express **13**, 7304–7318.

Grinberg, A. A., and S. Luryi, 1989, "Electron transmission across and interface of different one-dimensional crystals," Phys. Rev. B **39**, 7466–7475.

Guerrero, G., D. L. Boiko, and E. Kapon, 2004, "Photonic crystal heterostructures implemented with vertical-cavity surface-emitting lasers," Opt. Express **12**, 4922–4928.

Hafez, W., and M. Feng, 2005, "Experimental demonstration of pseudomorphic heterojunction bipolar transistors with cut-off frequencies above 600 GHz," Appl. Phys. Lett. **86**, 152101.

Heiblum, M., and M. V. Fischetti, 1990, "Ballistic hot-electron transistors," IBM J. Res. Dev. **34**, 530–549.

Ho, K. M., C. T. Chan, and C. M. Soukoulis, 1990, "Existence of a photonic gap in periodic dielectric structures," Phys. Rev. Lett. **65**, 3152–3155.

Hsue, Y. C., A. J. Freeman, and B. Y. Gu, 2005, "Extended plane-wave expansion method in three-dimensional anisotropic photonic crystals," Phys. Rev. B **72**, 195118.

Hsue, Y. C., and T. J. Yang, 2004, "Applying a modified plane-wave expansion method to the calculation of transmittivity and reflectivity of a semi-infinite photonic crystal," Phys. Rev. E **70**, 016706.

Istrate, E., M. Charbonneau-Lefort, and E. H. Sargent, 2002, "Theory of photonic crystal heterostructures," Phys. Rev. B **66**, 075121.

Istrate, E., A. A. Green, and E. H. Sargent, 2005, "Behavior of light at photonic crystal interfaces," Phys. Rev. B **71**, 195122.

Istrate, E., and E. H. Sargent, 2002, "The photonic analogue of the graded heterostructure: Analysis using the envelope approximation," Opt. Quantum Electron. **34**, 217–226.

Istrate, E., and E. H. Sargent, 2005a, "Measurement of the phase shift upon reflection from photonic crystals," Appl. Phys. Lett. **86**, 151112.

Istrate, E., and E. H. Sargent, 2005b, "Photonic crystal waveguide analysis using interface boundary conditions," IEEE J. Quantum Electron. **41**, 461–467.

Jiang, P., J. F. Bertone, K. S. Hwang, and V. L. Colvin, 1999a, "Single-crystal colloidal multilayers of controlled thickness," Chem. Mater. **11**, 2132–2140.

Jiang, P., N. Ostojic, R. Narat, D. M. Mittleman, and V. L. Colvin, 2001, "The fabrication and bandgap engineering of photonic multilayers," Adv. Mater. (Weinheim, Ger.) **13**, 389–393.

Jiang, W., R. T. Chen, and X. Lu, 2005, "Theory of light refraction at the surface of a photonic crystal," Phys. Rev. B **71**, 245115.

Jiang, Y., C. Niu, and D. L. Lin, 1999b, "Resonance tunneling through photonic quantum wells," Phys. Rev. B **59**, 9981–9986.

Jin, C., M. A. McLachlan, D. W. McComb, R. M. D. L. Rue, and N. P. Johnson, 2005, "Template-assisted growth of nominally cubic (100)-oriented three-dimensional crack-free photonic crystals," Nano Lett. **5**, 2646–2650.

Joannopoulos, J. D., R. D. Meade, and J. N. Winn, 1995, *Photonic Crystals: Molding the Flow of Light* (Princeton University Press, Princeton).

John, S., 1987, "Strong localization of photons in certain disordered dielectric superlattices," Phys. Rev. Lett. **58**, 2486–2489.

Johnson, S. G., S. Fan, A. Mekis, and J. D. Joannopoulos, 2001, "Multipole-cancellation mechanism for high-Q cavities in the absence of a complete photonic band gap," Appl. Phys. Lett. **78**, 3388–3390.

Johnson, S. G., S. Fan, P. R. Villeneuve, J. D. Joannopoulos, and L. A. Kolodziejski, 1999, "Guided modes in photonic crystal slabs," Phys. Rev. B **60**, 5751–5758.

Kalinina, O., and E. Kumacheva, 1999, "A "core-shell" approach to producing 3D polymer nanocomposites," Macromolecules **32**, 4122–4129.

Kane, E. O., 1957, "Band structure of indium antimonide," J. Phys. Chem. Solids **1**, 249–261.

Kawakami, S., 1997, "Fabrication of submicrometre 3D periodic structures composed of Si/SiO_2," Electron. Lett. **14**, 1260–1261.

Kawakami, S., T. Sato, K. Miura, Y. Ohtera, T. Kawashima, and H. Ohkubo, 2003, "3-D photonic-crystal hetero structures: Fabrication and in-line resonator," IEEE Photonics Technol. Lett. **15**, 816–818.

Kevorkian, J., 2000, *Partial Differential Equations: Analytical Solutions and Techniques* (Springer, New York).

Kohn, W., 1959, "Analytic properties of Bloch waves and Wannier functions," Phys. Rev. **115**, 809–821.

Kosaka, H., T. Kawashima, A. Tomita, M. Notomi, T. Tamamura, T. Sato, and S. Kawakami, 1998, "Superprism phenomena in photonic crystals," Phys. Rev. B **58**, R10096–R10099.

Kramper, P., M. Agio, C. M. Soukoulis, A. Birner, F. Müeller, R. B. Wehrspohn, U. Gösele, and V. Sandoghdar, 2004, "Highly directional emission from photonic crystal waveguides of subwavelength width," Phys. Rev. Lett. **92**, 113903.

Krauss, T. F., R. M. D. L. Rue, and S. Brand, 1996, "Two-dimensional photonic-bandgap structures operating at near-infrared wavelengths," Nature (London) **383**, 699–702.

Kroemer, H., 1957, "Theory of a wide-gap emitter for transistors," Proc. IRE **45**, 1535–1537.

Kroemer, H., 1963, "A proposed class of heterojunction injection lasers," Proc. IEEE **51**, 1782–1783.

Kroemer, H., 1982, "Heterostructure bipolar transistors and integrated circuits," Proc. IEEE **70**, 13–25.

Kumacheva, E., O. Kalinina, and L. Lilge, 1999, "Three dimensional arrays in polymer nanocomposites," Adv. Mater. (Weinheim, Ger.) **11**, 231–234.

Landon, P. B., *et al.*, 2003, "Inverse gold photonic crystals and conjugated polymer coated opals for functional materials," Physica B **338**, 165–170.

Lau, W. T., and S. Fan, 2002, "Creating large bandwidth line defects by embedding dielectric waveguides into photonic crystal slabs," Appl. Phys. Lett. **81**, 3915–3917.

Lenz, G., I. Talanina, and C. M. de Sterke, 1999, "Bloch oscillations in an array of curved optical waveguides," Phys. Rev. Lett. **83**, 963–966.

Li, L., 1996, "Formulation and comparison of two recursive matrix algorithms for modeling layered diffraction gratings," J. Opt. Soc. Am. A **13**, 1024–1035.

Li, Z.-Y., and K.-M. Ho, 2003, "Light propagation in semi-infinite photonic crystals and related waveguide structures," Phys. Rev. B **68**, 155101.

Li, Z.-Y., and L.-L. Lin, 2003, "Photonic band structures solved by a plane-wave-based transfer-matrix method," Phys. Rev. E **67**, 046607.

Lidorikis, E., P. T. Rakich, S. G. Johnson, J. D. Joannopoulos, E. P. Ippen, and H. I. Smith, 2004, "A three-dimensional optical photonic crystal with designed point defects," Nature (London) **429**, 538–542.

Lin, L.-L., and Z.-Y. Li, 2001, "Interface states in photonic crystal heterostructures," Phys. Rev. B **63**, 033310.

Lin, S. Y., E. Chow, S. G. Johnson, and J. D. Joannopoulos, 2000, "Demonstration of highly efficient waveguiding in a photonic crystal slab at the 1.5 micron wavelength," Opt. Lett. **25**, 1297–1299.

Lin, S.-Y., J. G. Fleming, R. Lin, M. M. Sigalas, R. Biswas, and K. M. Ho, 2001, "Complete three-dimensional photonic bandgap in a simple cubic structure," J. Opt. Soc. Am. B **18**, 32–35.

Lovell, P. A., and M. S. El-Asser, 1997, *Emulsion Polymerization and Emulsion Polymers* (Wiley, New York).

Lundeberg, L. D. A., D. L. Boiko, and E. Kapon, 2005, "Coupled islands of photonic crystal heterostructures implemented with vertical-cavity surface-emitting lasers," Appl. Phys. Lett. **87**, 241120.

Malpuech, G., A. Kavokin, G. Panzarini, and A. Di Carlo, 2001, "Theory of photon Bloch oscillations in photonic crystals," Phys. Rev. B **63**, 035108.

Meade, R. D., K. D. Brommer, A. M. Rappe, and J. D. Joannopoulos, 1991, "Electromagnetic Bloch waves at the surface of a photonic crystal," Phys. Rev. B **44**, 10961–10964.

Mingaleev, S. F., and K. Busch, 2003, "Scattering matrix approach to large-scale photonic crystal circuits," Opt. Lett. **28**, 619–621.

Mitin, V. V., V. A. Kochelap, and M. A. Stroscio, 1999, *Quantum Heterostructures—Microelectronics and Optoelectronics* (Cambridge University Press, Cambridge).

Miura, K., Y. Ohtera, H. Ohkubo, N. Akutsu, and S. Kawakami, 2003, "Reduction of propagation and bending losses of heterostructured photonic crystal waveguides by use of a high-delta structure," Opt. Lett. **28**, 734–736.

Momeni, B., and A. Adibi, 2003, "Optimization of photonic crystal demultiplexers based on the superprism effect," Appl. Phys. B **77**, 555–560.

Montie, E. A., E. C. Cosman, G. W. Hooft, M. B. van der Mark, and C. W. J. Beenakker, 1991, "Observation of the optical analogue of quantized conductance of a point contact," Nature (London) **350**, 594–595.

Moreno, E., F. J. García-Vidal, and L. Martín-Moreno, 2004, "Enhanced transmission spectrum of light via photonic crystal surface mode," Phys. Rev. B **69**, 121402(R).

Notomi, M., 2000, "Theory of light propagation in strongly modulated photonic crystals: Refraction like behavior in the vicinity of the photonic band gap," Phys. Rev. B **62**, 10696–10705.

Notomi, M., 2002, "Negative refraction in photonic crystals," Opt. Quantum Electron. **34**, 133–143.

Ochiai, T., and J. Sánchez-Dehesa, 2001, "Superprism effect in opal-based photonic crystals," Phys. Rev. B **64**, 245113.

Özbay, E., and B. Temelkuran, 1996, "Reflection properties and defect formation in photonic crystals," Appl. Phys. Lett. **69**, 743–745.

Painter, O., R. K. Lee, A. Scherer, A. Yariv, J. D. O'Brien, P. D. Dapkus, and I. Kim, 1999, "Two-dimensional photonic band-gap defect mode laser," Science **284**, 1819–1821.

Painter, O., and K. Srinivasan, 2003, "Localized defect states in two-dimensional photonic crystal slab waveguides: A simple model based upon symmetry analysis," Phys. Rev. B **68**, 035110.

Painter, O., K. Srinivasan, and P. E. Barclay, 2003, "Wannier-like equation for the resonant cavity modes of locally perturbed photonic crystals," Phys. Rev. B **68**, 035214.

Pendry, J. B., 1996, "Calculating photonic band structure," J. Phys.: Condens. Matter **8**, 1085–1108.

Pendry, J. B., and A. MacKinnon, 1992, "Calculation of photon dispersion relations," Phys. Rev. Lett. **69**, 2772–2775.

Poon, J., E. Istrate, M. Allard, and E. H. Sargent, 2003, "Multiple-scales analysis of photonic crystal waveguides," IEEE J. Quantum Electron. **39**, 778–786.

Ramos-Mendieta, F., and P. Halevi, 1999, "Surface electromagnetic waves in two-dimensional photonic crystals: Effect of the position of the surface plane," Phys. Rev. B **59**, 15112–15120.

Rengarajan, R., P. Jiang, D. C. Larrabee, V. L. Colvin, and D. M. Mittleman, 2001, "Colloidal photonic superlattices," Phys. Rev. B **64**, 205103.

Robbie, K., M. J. Brett, and A. Lakhtakia, 1996, "Chiral sculptured thin films," Nature (London) **384**, 616.

Robertson, W. M., G. Arjavalingam, R. D. Meade, K. D. Brommer, A. M. Rappe, and J. D. Joannopoulos, 1993, "Observation of surface photons on periodic dielectric arrays," Opt. Lett. **18**, 528–530.

Romanov, S. G., H. M. Yates, M. E. Pemble, and R. M. D. L. Rue, 2000, "Opal-based photonic crystal with double photonic bandgap structure," J. Phys.: Condens. Matter **12**, 8221–8229.

Roskos, H. G., M. C. Nuss, J. Shah, K. Leo, and D. A. B. Miller, 1992, "Coherent submillimeter-wave emission from charge oscillations in a double-well potential," Phys. Rev. Lett. **68**, 2216–2219.

Sai-Halasz, G. A., R. Tsu, and L. Esaki, 1977, "A new semiconductor superlattice," Appl. Phys. Lett. **30**, 651–653.

Sakaki, H., 1982, "Velocity-modulation transistor (VMT)—A new field-effect transistor concept," Jpn. J. Appl. Phys., Part 2 **21**, L381–L383.

Sakoda, K., 1995a, "Optical transmittance of a two-dimensional triangular photonic lattice," Phys. Rev. B **51**, 4672–4675.

Sakoda, K., 1995b, "Symmetry, degeneracy and uncoupled modes in two-dimensional photonic lattices," Phys. Rev. B **52**, 7982–7986.

Sato, T., K. Miura, N. Ishino, Y. Ohtera, T. Tamamura, and S. Kawakami, 2002, "Photonic crystals for the visible range fabricated by autocloning technique and their application," Opt. Quantum Electron. **34**, 63–70.

Schroden, R. C., M. Al-Daous, C. F. Blanford, and A. Stein, 2002, "Optical properties of inverse opal photonic crystals," Chem. Mater. **14**, 3305–3315.

Sharkawy, A., S. Shi, and D. W. Prather, 2002, "Heterostructure photonic crystals: Theory and applications," Appl. Opt. **41**, 7245–7253.

Sharma, B. L., and R. K. Purohit, 1974, *Semiconductor Heterojunctions* (Pergamon, Oxford).

Sipe, J. E., 2000, "Vector $k \cdot p$ approach for photonic crystal band structures," Phys. Rev. E **62**, 5672–5677.

Smith, D. L., and C. Mailhiot, 1986, "$k \cdot p$ theory of semiconductor superlattice electronic structure. I. Formal results," Phys. Rev. B **33**, 8345–8359.

Smith, D. L., and C. Mailhiot, 1990, "Theory of semiconductor superlattice electronic structure," Rev. Mod. Phys. **62**, 173–234.

Song, B. S., T. Asano, and Y. Akahane, 2004, "Transmission and reflection characteristics of in-plane hetero-photonic crystals," Appl. Phys. Lett. **85**, 4591–4593.

Song, B. S., T. Asano, Y. Akahane, and S. Noda, 2005a, "Role of interfaces in heterophotonic crystals for manipulation of photons," Phys. Rev. B **71**, 195101.

Song, B. S., T. Asano, Y. Akahane, Y. Tanaka, and S. Noda, 2005b, "Multichannel add/drop filter based on in-plane hetero photonic crystals," J. Lightwave Technol. **23**, 1449–1455.

Song, B. S., S. Noda, and T. Asano, 2003, "Photonic devices based on in-plane hetero photonic crystals," Science **300**, 1537.

Song, B. S., S. Noda, T. Asano, and Y. Akahane, 2005, "Ultra-high-Q photonic double-heterostructure nanocavity," Nat. Mater. **4**, 207–210.

Souza, I., N. Marzari, and D. Vanderbilt, 2002, "Maximally localized Wannier functions for entangled energy bands," Phys. Rev. B **65**, 035109.

Srinivasan, K., P. Barclay, M. Borselli, and O. Painter, 2004, "Optical-fiber-based measurement of an ultrasmall volume high-Q photonic crystal microcavity," Phys. Rev. B **70**, 081306(R).

Srinivasan, K., P. Barclay, O. Painter, J. Chen, A. Cho, and C. Gmachl, 2003, "Experimental demonstration of a high quality factor photonic crystal microcavity," Appl. Phys. Lett. **83**, 1915–1917.

Srinivasan, K., P. E. Barclay, and O. Painter, 2004, "Fabrication-tolerant high quality factor photonic crystal microcavities," Opt. Express **12**, 1458–1463.

Srinivasan, K., and O. Painter, 2002, "Momentum space design of high-Q photonic crystal optical cavities," Opt. Express **10**, 670–684.

Srinivasan, K., and O. Painter, 2003, "Fourier space design of high-Q cavities in standard and compressed hexagonal lattice photonic crystals," Opt. Express **11**, 579–593.

Stefanou, N., V. Karathanos, and A. Modinos, 1992, "Scattering of electromagnetic waves by periodic structures," J. Phys.: Condens. Matter **4**, 7389–7400.

Stefanou, N., V. Yannopapas, and A. Modinos, 1998, "Heterostructures of photonic crystals: Frequency bands and transmission coefficients," Comput. Phys. Commun. **113**, 49–77.

Stefanou, N., V. Yannopapas, and A. Modinos, 2000, "MULTEM 2: A new version of the program for transmission and

band-structure calculations of photonic crystals," Comput. Phys. Commun. **132**, 189–196.

Stöber, W., A. Fink, and E. Bohn, 1968, "Controlled growth of monodisperse silica spheres in micron size range," J. Colloid Interface Sci. **26**, 62–69.

Suzuki, T., and K. L. Yu, 1995, "Tunneling in photonic band structures," J. Opt. Soc. Am. B **12**, 804–820.

Taflove, A., and S. C. Hagness, 2000, *Computational Electrodynamics: The Finite-Difference Time-Domain Method* (Artech House, Norwood, MA).

Takano, H., B. S. Song, T. Asano, and S. Noda, 2005, "Highly efficient in-plane channel drop filter in a two-dimensional heterophotonic crystal," Appl. Phys. Lett. **86**, 241101.

Tokushima, M., H. Yamada, and Y. Arakawa, 2004, "1.5 μm wavelength light guiding in waveguides in square-lattice-of-rod photonic crystal slab," Appl. Phys. Lett. **84**, 4298–4300.

Tsang, W. T., 1982, "Extremely low threshold (AlGa)As graded-index waveguide separate-confinement heterostructure lasers grown by molecular beam epitaxy," Appl. Phys. Lett. **40**, 217–219.

van Blaaderen, A., and A. Vrij, 1993, "Synthesis and characterization of monodisperse colloidal organo-silica spheres," J. Colloid Interface Sci. **156**, 1–18.

van Haeringen, W., and D. Lenstra, 1990, *Analogies in Optics and Micro Electronics* (Kluwer Academic, Dordrecht).

van Wees, B. J., H. van Houten, C. W. J. Beenakker, J. G. Williamson, L. P. Kouwenhoven, D. van der Marel, and C. T. Foxon, 1988, "Quantized conductance of pint contacts in a two-dimensional electron gas," Phys. Rev. Lett. **60**, 848–850.

Vekris, E., V. Kitaev, G. von Freymann, D. D. Perovic, J. S. Aitchison, and G. A. Ozin, 2005, "Buried linear extrinsic defects in colloidal photonic crystals," Adv. Mater. (Weinheim, Ger.) **17**, 1269–1272.

Velev, O. D., T. A. Jede, R. F. Lobo, and A. M. Lenhoff, 1997, "Porous silica via colloidal crystallization," Nature (London) **389**, 447–448.

Velev, O. D., and E. W. Kaler, 2000, "Structured porous materials via colloidal crystal templating: From inorganic oxides to metals," Adv. Mater. (Weinheim, Ger.) **12**, 531–534.

Vlasov, Y. A., X. Z. Bo, J. C. Sturm, and D. J. Norris, 2001, "On-chip natural assembly of silicon photonic bandgap crystals," Nature (London) **414**, 289–293.

Vlasov, Y. A., N. Moll, and S. J. McNab, 2004, "Observation of surface states in a truncated photonic crystal slab," Opt. Lett. **29**, 2175–2177.

Wang, X., X. Hu, Y. Li, W. Jia, C. Xu, X. Liu, and J. Zi, 2002, "Enlargement of omnidirectional total reflection frequency range in one-dimensional photonic crystals by using photonic heterostructures," Appl. Phys. Lett. **80**, 4291–4293.

Wannier, G. H., 1962, "Dynamics of band electrons in electric and magnetic fields," Rev. Mod. Phys. **34**, 645–655.

Waschke, C., H. G. Roskos, R. Schwedler, K. Leo, H. Kurz, and K. Köhler, 1993, "Coherent submillimeter-wave emission from Bloch oscillations in a semiconductor superlattice," Phys. Rev. Lett. **70**, 3319–3322.

Weisbuch, C., and B. Vinter, 1991, *Quantum Semiconductor Structures: Fundamentals and Applications* (Academic, Boston).

Wijnhoven, J. E. G. J., and W. L. Vos, 1998, "Preparation of photonic crystals made of air spheres in titania," Science **281**, 802–804.

Wilkinson, P. B., 2002, "Photonics Bloch oscillations and Wannier-Stark ladders in exponentially chirped Bragg gratings," Phys. Rev. E **65**, 056616.

Wong, S., V. Kitaev, and G. A. Ozin, 2003, "Colloidal crystal films: Advances in universality and perfection," J. Am. Chem. Soc. **125**, 15589–15598.

Wu, L., M. Mazilu, T. Karle, and T. F. Krauss, 2002, "Superprism phenomena in planar photonic crystals," IEEE J. Quantum Electron. **38**, 915–918.

Xia, Y., B. Gates, Y. Yin, and Y. Lu, 2000, "Monodispersed colloidal spheres: Old materials with new applications," Adv. Mater. (Weinheim, Ger.) **12**, 693–713.

Xu, T., S. Yang, S. V. Nair, and H. E. Ruda, 2005, "Confined modes in finite-size photonic crystals," Phys. Rev. B **72**, 045126.

Yablonovitch, E., 1987, "Inhibited spontaneous emission in solid-state physics and electronics," Phys. Rev. Lett. **58**, 2059–2062.

Yablonovitch, E., T. J. Gmitter, and K. M. Leung, 1991, "Photonic band structure: The face-centered-cubic case employing nonspherical atoms," Phys. Rev. Lett. **67**, 2295–2298.

Yan, Q., A. Chen, S. J. Chua, and X. S. Zhao, 2005, "Incorporation of point defects into self-assembled three-dimensional colloidal crystals," Adv. Mater. (Weinheim, Ger.) **17**, 2849–2853.

Yan, Q., Z. Zhou, X. S. Zhao, and S. J. Chua, 2005, "Line defects embedded in three-dimensional photonic crystals," Adv. Mater. (Weinheim, Ger.) **17**, 1917–1920.

Yang, S., T. Xu, H. Ruda, and M. Cowan, 2005, "Numerical study of anomalous refraction in photonic crystals," Phys. Rev. B **72**, 075128.

Yannopapas, V., N. Stefanou, and A. Modinos, 2001, "Effect of stacking faults on the optical properties of inverted opals," Phys. Rev. Lett. **86**, 4811–4814.

Yano, S., Y. Segawa, J. S. Bae, K. Mizuno, H. Miyazaki, K. Ohtaka, and S. Yamaguchi, 2001, "Quantized state in a single quantum well structure of photonic crystals," Phys. Rev. B **63**, 153316.

Yariv, A., and P. Yeh, 1984, *Waves in Crystalline Media* (Wiley, New York).

Ye, Y. H., S. Badilescu, and V. V. Truong, 2002, "Large-scale ordered macroporous SiO_2 thin films by a template-directed method," Appl. Phys. Lett. **81**, 616–618.

Yee, K. S., 1966, "Numerical solution of initial boundary value problems involving Maxwell's equations in isotropic media," IEEE Trans. Antennas Propag. **14**, 302–307.

Yeh, P., 1988, *Optical Waves in Periodic Media* (Wiley, New York).

Yu, X., and S. Fan, 2004, "Anomalous reflections at photonic crystal surfaces," Phys. Rev. E **70**, 055601(R).

Zhang, C., F. Qiao, and J. Wan, 2000, "Enlargement of non-transmission frequency range in photonic crystals by using multiple heterostructures," J. Appl. Phys. **87**, 3174–3176.

Zhu, Q. G., and H. Kroemer, 1983, "Interface connection rules for effective-mass wave functions at an abrupt heterojunction between two different semiconductors," Phys. Rev. B **27**, 3519–3527.